American Society of Hematology
2021 L Street NW, Suite 900,
Washington, DC 20036
Phone: 202-776-0544 | Fax 202-776-0545
editorial@hematology.org

Overexpression of wild type IL-7Rα promotes T-cell acute lymphoblastic leukemia/lymphoma

Tracking no: BLD-2019-000553R2

Ana Patricia Silva (Roche innovation center basel, Switzerland) Afonso Almeida (Instituto de Medicina Molecular João Lobo Antunes, Faculdade de Medicina, Universidade de Lisboa, Portugal) Ana Cachucho (Instituto de Medicina Molecular João Lobo Antunes, Faculdade de Medicina, Universidade de Lisboa, Portugal) João Neto (Instituto de Medicina Molecular João Lobo Antunes, Faculdade de Medicina, Universidade de Lisboa, Portugal) Sofie Demeyer (VIB / KULeuven, Belgium) Mafalda Ramos de Matos (Instituto de Medicina Molecular João Lobo Antunes, Faculdade de Medicina, Universidade de Lisboa, Portugal) Thea Hogan (Institute of Immunity and Transplantation, Division of Infection and Immunity, University College London, United Kingdom) Yunlei Li (Erasmus Medical Center-Sophia Children's Hospital, Netherlands) Jules Meijerink (Princess Máxima Center for Pediatric Oncology, Netherlands) Jan Cools (KU Leuven Center for Human Genetics, Leuven, Belgium, Belgium) Ana Grosso (UCIBIO, Departamento de Ciências da Vida, Faculdade de Ciências e Tecnologia, Universidade NOVA de Lisboa, Portugal) Benedict Seddon (University College London, United Kingdom) Joao Barata (Instituto de Medicina Molecular João Lobo Antunes, Faculdade de Medicina, Universidade de Lisboa, Portugal)

Abstract:
Tight regulation of IL-7Rα expression is essential for normal T-cell development. IL-7Rα gain-of-function mutations are known drivers of T-cell acute lymphoblastic leukemia (T-ALL). Although a subset of T-ALL patients display very high *IL7R* mRNA levels and cases with *IL7R* gains have been reported, the impact of IL-7Rα overexpression, rather than mutational activation, on leukemogenesis remains unclear. Here, we show that overexpression of IL-7Rα in tetracycline-inducible *Il7r* transgenic and Rosa26 *IL7R* knock-in mice drives potential thymocyte self-renewal, and thymus hyperplasia due to increased proliferation of T-cell precursors, which subsequently infiltrate lymph nodes, spleen and bone marrow, ultimately leading to fatal leukemia. The tumors mimic key features of human T-ALL, including heterogeneity in immunophenotype and genetic subtype between cases, frequent hyperactivation of PI3K/Akt pathway that is paralleled by downregulation of $p27^{Kip1}$ and upregulation of Bcl-2, and gene expression signatures evidencing JAK/STAT, PI3K/Akt/mTOR and Notch signaling activation. Notably, we also find that established tumors may no longer require high levels of IL-7R expression upon secondary transplantation and can progress in the absence of IL-7, but remain sensitive to inhibitors of IL-7R-mediated signaling Ruxolitinib (Jak1), AZD1208 (Pim), Dactolisib (PI3K/mTOR), Palbociclib (Cdk4/6), and Venetoclax (Bcl-2). The relevance of these findings for human disease are highlighted by the fact that T-ALL patient samples with high wild type *IL7R* expression display a transcriptional signature resembling that from IL-7-stimulated pro-T cells and, critically, from *IL7R* mutant T-ALL cases. Overall, our studies demonstrate that high expression of IL-7Rα can promote T-cell tumorigenesis even in the absence of IL-7Rα mutational activation.

Conflict of interest: No COI declared

COI notes:

Preprint server: No;

Author contributions and disclosures: AS and AA designed and performed experiments, analyzed and interpreted data; AC and TH performed experiments; JLN, MM, SD and YL conducted bioinformatics analyses; JM, JC and ARG supervised the bioinformatics analyses and provided critical suggestions and feedback; BS and JTB designed research, analyzed and interpreted data, supervised the studies and wrote the manuscript. All authors critically read and contributed to the final version of the manuscript.

Non-author contributions and disclosures: No;

Agreement to Share Publication-Related Data and Data Sharing Statement: RNA-seq data for mouse tumor and control samples is available at GEO under accession number GSE128212.

Clinical trial registration information (if any):

Overexpression of wild type IL-7Rα promotes T-cell acute lymphoblastic leukemia/lymphoma

Ana Silva[1,2,3#], Afonso Almeida[2#], Ana Cachucho[2**], João L. Neto[2**], Sofie Demeyer[4], Mafalda Matos[2], Thea Hogan[1], Yunlei Li[5], Jules Meijerink[6], Jan Cools[4], Ana Rita Grosso[7], Benedict Seddon[1]* and João T. Barata[2]*

[1]Institute of Immunity and Transplantation, Division of Infection and Immunity, University College London; [2]Instituto de Medicina Molecular João Lobo Antunes, Faculdade de Medicina, Universidade de Lisboa, Lisbon, Portugal; [3]Current address: Roche Pharma Research and Early Development, Pharmaceutical Sciences, Roche Innovation Center Basel, F. Hoffmann-La Roche Ltd., Grenzacherstrasse 124, 4070 Basel, Switzerland; [4]VIB Center for Cancer Biology & KU Leuven Center for Human Genetics, VIB - KU Leuven, Leuven, Belgium; [5]Erasmus Medical Center Rotterdam, Department of Pathology, Rotterdam, Netherlands; [6]Princess Máxima Center for Pediatric Oncology, Utrecht, Netherlands.; [7]UCIBIO, Departamento de Ciências da Vida, Faculdade de Ciências e Tecnologia, Universidade NOVA de Lisboa, 2829-516 Caparica, Portugal.

* BS and JTB contributed equally to this work

AS and AA are joint first authors

** AC and JLN are joint second authors

Correspondence to:

Benedict Seddon, Institute of Immunity and Transplantation, Division of Infection and Immunity, University College London, Royal Free Hospital, Rowland Hill Street, London NW3 2PF, England, UK; Tel: +44 2077940500; e-mail: benedict.seddon@ucl.ac.uk; or to:

João T. Barata, Instituto de Medicina Molecular João Lobo Antunes, Lisbon University Medical School, Av. Prof. Egas Moniz, 1649-028 Lisboa, Portugal; Tel: +351217999524; e-mail: joao_barata@medicina.ulisboa.pt

Running title: Elevated IL-7Rα promotes T-cell leukemia

Key Points

• Mice overexpressing wild type IL-7Rα develop leukemia with features of human T-ALL, and sensitivity to ruxolitinib, dactolisib and venetoclax

• T-ALL patients with high levels of wild type *IL7R* present with evidence of ongoing, oncogenic-like IL-7R-mediated signaling activation.

Abstract

Tight regulation of IL-7Rα expression is essential for normal T-cell development. IL-7Rα gain-of-function mutations are known drivers of T-cell acute lymphoblastic leukemia (T-ALL). Although a subset of T-ALL patients display very high *IL7R* mRNA levels and cases with *IL7R* gains have been reported, the impact of IL-7Rα overexpression, rather than mutational activation, on leukemogenesis remains unclear. Here, we show that overexpression of IL-7Rα in tetracycline-inducible *Il7r* transgenic and Rosa26 *IL7R* knock-in mice drives potential thymocyte self-renewal, and thymus hyperplasia due to increased proliferation of T-cell precursors, which subsequently infiltrate lymph nodes, spleen and bone marrow, ultimately leading to fatal leukemia. The tumors mimic key features of human T-ALL, including heterogeneity in immunophenotype and genetic subtype between cases, frequent hyperactivation of PI3K/Akt pathway that is paralleled by downregulation of $p27^{Kip1}$ and upregulation of Bcl-2, and gene expression signatures evidencing JAK/STAT, PI3K/Akt/mTOR and Notch signaling activation. Notably, we also find that established tumors may no longer require high levels of IL-7R expression upon secondary transplantation and can progress in the absence of IL-7, but remain sensitive to inhibitors of IL-7R-mediated signaling Ruxolitinib (Jak1), AZD1208 (Pim), Dactolisib (PI3K/mTOR), Palbociclib (Cdk4/6), and Venetoclax (Bcl-2). The relevance of these findings for human disease are highlighted by the fact that T-ALL patient samples with high wild type *IL7R* expression display a transcriptional signature resembling that from IL-7-stimulated pro-T cells and, critically, from

IL7R mutant T-ALL cases. Overall, our studies demonstrate that high expression of IL-7Rα can promote T-cell tumorigenesis even in the absence of IL-7Rα mutational activation.

Introduction

Interleukin 7 (IL-7) and its receptor, a heterodimer constituted by IL-7Rα (encoded by *IL7R*) and γc (encoded by *IL2RG*) subunits, are essential for normal T-cell development and homeostasis [1-4], with *IL7R* genetic inactivation leading to severe combined immunodeficiency [5]. Contrarily, *IL7R* gain-of-function mutations, which occur in roughly 10% of T-cell acute lymphoblastic leukemia (T-ALL) patients, are considered drivers of leukemia, being largely mutually exclusive with other mutations affecting downstream IL-7R signaling components, including JAK1/3, STAT5B, PTEN and Akt [6-13]. In agreement with an oncogenic role for excessive IL-7/IL-7R signaling, IL-7 transgenic mice develop lymphomas [14] and xenotransplant models of human T-ALL rely on microenvironmental IL-7 for tumor acceleration [15]. Moreover, IL-7 prevents spontaneous apoptosis and promotes proliferation of T-ALL cells *in vitro* [16-20] in large part by activating JAK/STAT5 and PI3K/Akt/mTOR signaling pathways, consequently promoting glucose uptake, upregulating Bcl-2 and downregulating the cyclin-dependent kinase inhibitor $p27^{kip1}$ [16,21-25]. These studies highlight the importance of keeping IL-7/IL-7R-mediated signaling levels within strict boundaries and, indeed, IL-7Rα expression at the cell surface is tightly regulated throughout both human and mouse T-cell development [1,4].

However, although *IL7R* gene amplification has been reported in T-ALL [26,27], its functional consequences have not been explored and it is not known whether high levels of wild type IL-7Rα are oncogenic *per se*. Here, we show that forced expression of wild type IL-7Rα in tetracycline-inducible *Il7r* transgenic or Rosa26 *IL7R* knock-in mice promotes widespread leukemia/lymphoma with features that resemble human T-ALL, and that pediatric T-ALL patient samples with high levels of wild type *IL7R* display an IL-7R-mediated gene expression profile similar to that observed in IL-7-activated pro-T cells and, notably, in cases with oncogenic *IL7R* gain-of-function mutations. These results provide strong evidence, arising from two different mouse models and

from human T-ALL patient samples, that high expression of IL-7Rα can contribute to T-ALL even in the absence of mutational activation of the receptor.

Methods

Mouse models. TreIL7R rtTA.C IL7rKO (TetIL-7R) tetracycline inducible IL-7R transgenic mice have been previously described [28]. TCR transgenes were introduced to the TetIL-7R background by intercrossing with Class I restricted F5 TCR transgenic and Class II restricted OTII transgenic lines to generate F5 TetIL-7R, F5 Rag1KO TetIL-7R and OTII TetIL-7R strains. Mice were fed doxycycline (dox) in food (3 mg/g) to induce IL-7Rα expression. Rosa26 *IL7R* (Rosa26-hIL-7R.huCD2-Cre) mice were generated as follows. We generated a conditional loxP-STOP-human *IL7R* knock-in mouse line under the control of the ubiquitous *Rosa26* promoter in C57Bl6 background. Homozygous animals were bred with CD2iCre animals [29] in order to promote expression of human *IL7R* in T cells. CD2-expressing F1 animals were viable and bred again with homozygous conditional animals in order to generate animals carrying two alleles of the knocked-in human *IL7R*. $CD2^{neg}$ $hIL7R^{+/+}$ and $CD2^{neg}$ $hIL7R^{+/-}$ animals were used as controls. Experimental mice were weekly weighed and sacrificed in a CO_2 chamber or via pentobarbital injection when presenting clear disease symptoms, with a defined endpoint of loss of 20% of body weight, breathing impairment, poor reaction to external stimuli and ruff fur appearance. Disseminated disease was confirmed minimally by analyzing thymus and spleen of mice. Differences in survival curves were determined by Log-rank (Mantel-Cox) test using Prism v6.0. All animals were bred and kept in specific pathogen-free (SPF) facilities at NIMR or IMM-JLA and experiments were performed according to the UCL Animal Welfare and Ethical Review Body and Home Office regulations, UK, and IMM-JLA's institutional and Portuguese (DGAV) regulations.

Organ analysis. Animals were dissected and organs were mechanically disintegrated into single cell suspensions in RPMI/ 2%(w/v) BSA (RPMI/BSA). Bone marrow was extracted by flushing off or crushing long bones (femur). Cell numbers were determined using an automated cell counter

(CASY 1, Scharfe System, Reutlingen, Germany) and cells subsequently transferred, immunophenotyped or lysed for immunoblotting as described below.

Adoptive transfers. To assess the malignancy of thymus-recovered cells, $10x10^6$ cells/ 250µl IMDM/BSA were injected via tail vein into 6-8 week-old *Rag1*$^{-/-}$ animals. Animals were fed with 3mg/g dox-containing food. Animals were monitored daily and sacrificed in a CO_2 chamber when moribund or at indicated time points. Bones, spleen and thymus were collected for flow cytometry and histological analysis. $4x10^5$ leukemic cells from the Hu-IL7Rα expressing model were transferred *i.v.* into sex and age-matched *Rag2*$^{-/-}\gamma_c^{-/-}$ and *Rag2*$^{-/-}\gamma_c^{-/-}$*Il7*$^{-/-}$ mice. Animals were monitored daily and sacrificed via pentobarbital injection when moribund. Bones, spleen and thymus were collected for flow cytometry and histological analysis.

Immunophenotype. Splenic, thymic and bone marrow cell suspensions were subjected to immunophenotypic analysis using standard methodology. Briefly, $2\text{-}5x10^5$ cells were stained for 20 minutes at 4ºC in PBS with 2%BSA with specific antibodies. Phycoerythrin (PE)–conjugated antibody against human IL-7Rα from R&D or ebioscience, and Per-CP, PE-Cy7, APC, APC-Cy7, BV421, BV510, BV605 and BV710 conjugated antibody against CD4, CD5, CD45, CD8, CD44, CD25, CD3 or TCRβ (H57-597), all from Biolegend were used in diverse combinations. When Lineage positive cells were excluded, biotin coupled anti- Gr-1, CD11b, CD19, Ter119 and CD11c were used and subsequently stained with BV711 streptavidin. Intracellular staining for Ki67 (APC-conjugated, Biolegend) or Bcl-2 (PE-conjugated, Biolegend) was performed using the Foxp3 staining kit from ebiosciences. 8 and 10-color analyses were performed on LSR Fortessa II (Becton Dickinson San Jose, CA, USA) flow cytometers. Results were analyzed with FlowJo (Tree Star Inc., Ashland, OR, USA) software.

Immunoblotting. Cells were lysed as described elsewhere [21]. Equal amounts of protein (50 μg/sample) were analyzed by 10% SDS-PAGE, transferred onto nitrocellulose membranes, and immunoblotted with the antibodies at 1:1000 dilution: $p27^{Kip1}$, actin (Santa Cruz Biotechnology, Santa Cruz, CA, USA), PTEN and p-Akt (S473) (Cell Signaling Technology, Danvers, MA, USA). Immunodetection was performed by incubation with horseradish peroxidise-conjugated anti-mouse (1:5000), anti-rabbit IgG (1:10,000) or anti-goat (1:5000) (Promega, Madison, WI, USA) and developed by enhanced chemiluminescence (Amersham-Pharmacia, Piscataway, NJ, USA).

Mouse transcriptome data. PolyA+ RNA-seq libraries of mouse tumors and normal samples were sequenced as paired-end 75-bp reads using standard Illumina pipeline. Data quality was assessed with the FastQC (http://www.bioinformatics.babraham.ac.uk/projects/fastqc/). Gene expression levels were determined by mapping RNA-seq reads to the mouse genome (mm10) with Kallisto v.2.8.4 [30]. Comparative transcriptome analysis between mouse tumors and human T-ALL was performed using previously published microarray data [31]. First, the raw microarray data were normalized and summarized with the Robust MultiArray Average method as implemented in the 'affy' package [32] from R (https://www.r-project.org/). Second, Human-Mouse orthologues were obtained from Ensembl v95 through 'biomaRt' R package [33]. Third, human microarray data and mouse RNA-seq expression levels were centered and scaled to remove technical bias. Finally, similarity between human and mouse transcriptome profiles were assessed by Pearson correlation, using previously defined gene signatures for human T-ALL sub-groups [31]. The correlation coefficients were graphically represented through an unsupervised clustering heatmap. To evaluate signaling pathways affected in tumors we used the GSEA tool [34] and KEGG gene sets from the Molecular Signature Database. This analysis was based on the moderated T-test values between tumor and normal samples estimated from voom transformed values as implemented in 'limma' R package [35].

Data Sharing Statement. RNA-seq data for mouse tumor and control samples is available at GEO under accession number GSE128212. WES data for tumor and control samples is available at SRA under accession number (under submission).

Additional methodological details in Supplementary Data online.

Results

Overexpression of IL-7Rα perturbs normal T-cell development in young *Il7r* transgenic mice

To evaluate whether high levels of IL-7Rα expression are sufficient to promote T-cell leukemia development, we first used a mouse model in which expression of an *Il7r* transgene, in an *Il7r*-null background, is induced in T lineage cells by a tetracycline responsive promotor (TreIl7r rtTA^{huCD2} *Il7r*$^{-/-}$ mice [28]; hereafter referred to as TetIL-7R). Consistent with earlier studies [28], young adult TetIL-7R animals continuously fed doxycycline from birth (TetIL-7R^{ON}) displayed some rescue of peripheral T-cell reconstitution compared with dox free mice (TetIL-7R^{OFF}) in line with the requirement of IL-7R signaling for normal thymopoiesis (**Fig. S1A**). However, thymi showed evidence of perturbed development, with increased frequency of immature TCR^{lo} CD8 single positive (ISP) thymocytes (**Fig. S1B**). This possibly reflects a partial differentiation block at the ISP stage, which would be in accordance with exacerbated IL-7R-mediated signaling during beta-selection [36]. Interestingly, mice transplanted with bone marrow progenitor cells expressing JAK3 mutants display a similar accumulation of ISP CD8+ cells [37], in line with JAK3 being downstream of IL-7-mediated signals. Inducible IL-7Rα expression was particularly elevated on the CD8 ISP population and a subset of DP thymocytes (**Fig. S1C**). Elevated IL-7Rα levels were associated with increased cell size (**Fig. S2A**) and increased proliferation, as assessed both by DNA content (**Fig. S2B**) and Ki67 expression (**Fig. S2C**). Of significance, DNA content distribution indicated that immature CD8 SP thymocytes in TetIL-7R^{ON} mice were highly proliferative (**Fig. S2B**). Accordingly, the Ki67 profile of TetIL-7R^{ON} CD8SP cells resembled that of WT ISP, which are known to have very high division rates, and not of mature WT CD8SP that exhibit much less proliferation (**Fig. S2C**).

TetIL-7R mice display progressive thymic hyperplasia and eventually develop fatal T-cell leukemia/lymphoma

To assess the consequence of abnormal thymic development in TetIL-7R mice, we analyzed lymphoid compartments in TetIL-7R strains [28] over time. Ageing is usually associated with thymic atrophy [38,39] as confirmed in the controls (**Fig. 1A**). Instead, TetIL7R^{ON} strains exhibited progressive increases in thymic cellularity with age (**Fig. 1A**). Hyperplasia was associated with a broad range of aberrant phenotypes that eventually spread to peripheral lymphoid tissues, as hyperplasia progressed to full-blown leukemia/lymphoma (**Fig. 1B**). Disseminated disease was also associated with hyperproliferation in both thymus and periphery, as assessed by Ki67 expression (**Fig. 1C**). A majority of the mice (90%) eventually died of late-onset fatal leukemia/lymphoma (**Fig. 1D**), with kinetics resembling those of other major T-cell oncogenes such as TAL1 or LMO2 [40,41]. Importantly, disease progression was dependent upon induced TetIL-7R expression, since TetIL-7R mice that were not dox fed as well as control mice that lack the rtTA driver transgene remained healthy. Moreover, disease was transferrable, confirming its malignant nature. Adoptive transfer of thymic cells from TetIL-7R mice with evidence of disseminated leukemia/lymphoma (**Fig. 1E**) to immunodeficient *Rag1*$^{-/-}$ mice resulted in the rapid onset of disease in all recipients (not shown), which displayed a similar pattern of lymphoid organ infiltration as the host, including bone marrow (**Fig. 1F**). Bone marrow involvement and widespread disease are characteristic features of advanced-stage T-ALL.

Given the oncogenic potential displayed by high IL-7R expression, we next addressed whether IL-7R overexpression could engage a self-renewal program prior to leukemia development. We removed TetIL-7R mice from dox at 8 weeks of age and analyzed their phenotype 12 weeks after dox removal. Out of 14 animals, 1 displayed near-normal thymic T-cell distribution, 6 showed signs of pre-leukemia (aberrant T-cell development with evidence of differentiation blockade) and 2 developed leukemia, altogether suggesting that self-renewal was engaged by *Il7r* overexpression before 8 weeks in a majority of the cases (**Fig. S3**). The remaining

off-dox mice did not display (abnormal) T cell development or signs of disease, indicating that removal of IL7R early on can, in a minority of the cases, prevent T cell precursor self-renewal and leukemogenesis. As expected, all mice that were kept on dox (n=17) displayed an aberrant phenotype or full blown leukemia at 12 weeks or earlier (**Fig. S3**). Altogether, our data suggest that IL-7Rα overexpression may engage a self-renewal program in T cell precursors, which is established by 8 weeks of age in a majority of the cases, eventually leading to subsequent leukemia development.

Leukemia development downstream from IL-7R is influenced by Rag1 expression but not by TCR signaling

Triggering TCR-dependent signaling in T-ALL using high-affinity self-peptide/MHC or anti-CD3 monoclonal antibodies was recently shown to induce apoptosis of T-ALL cells [42], demonstrating the therapeutic potential of activating TCR signals in this malignancy. The relevance of TCR-mediated signaling for T-ALL development is less clear. Since IL-7R expression in TetIL-7R^{ON} mice was maximal in immature SP and DP thymocytes, we asked whether TCR-dependent thymic selection signaling could impact on the development of the disease. To assess this, we compared disease progression of TetIL-7R mice on a polyclonal *Tcr* background with strains expressing either Class I- or Class II-restricted TCR transgenes (F5 and OTII, respectively). In polyclonal mice, only a small fraction of DPs receive stronger TCR signals compatible with selection, while in TCR transgenic mice, all cells express TCRs capable of onward development. Despite this, disease progression in the three strains revealed a near identical kinetics of disease development, irrespective of TCR specificity (**Fig. 2A**), arguing against a major role for TCR signaling in modulating IL-7R-dependent leukemogenesis. This is in line with what has been reported for STAT5 [43] transgenic mice, in which modulation of TCR expression did not affect leukemia/lymphoma development.

The contribution of Rag activity for T-cell leukemogenesis has long been recognized, including in the context of TCR recombination-driven chromosomal reciprocal translocations displayed by T-ALL patients, and recently highlighted as highly involved in leukemogenesis in ETV6-RUNX1-positive B-cell ALL [44]. Also, we previously showed that T-ALL-associated PTEN microdeletions resulting in loss of PTEN expression are RAG-mediated [45]. Because some of the tumors displayed low or absent PTEN protein levels, we analyzed the requirement of RAG activity for IL-7R-mediated tumor development. RAGs are essential for *TCR* gene rearrangement and subsequent T-cell development past the DN stages. As such, lack of RAG activity could affect T-ALL development merely because it prevented thymocyte differentiation. To avoid this confounding factor, we analyzed TCR-transgenic F5 mice which do not require RAG activity for T cell maturation in the thymus. Comparison of F5 TetIL-7R *Rag1*$^{-/-}$ and F5 TetIL-7R mice revealed that absence of *Rag1* expression significantly delayed, although it did not fully prevent, tumor development (**Fig. 2B**). This suggests that RAG activity contributes to leukemia acceleration, although it is not absolutely required for leukemia development downstream from IL-7R overexpression in T-cell precursors.

Maintenance of established TetIL-7R tumors may occur in the absence of high IL-7Rα

Making use of our inducible model, we next assessed whether IL-7Rα expression was required for maintenance and expansion of established tumors. Malignant cells isolated from 3 independent primary F5 TetIL-7R tumors were transferred into *Rag1*$^{-/-}$ recipient mice either fed doxycycline (on-dox), to maintain *Il7r* expression, or maintained dox free, to cease gene induction. Both groups of mice were culled 4 weeks posttransplant due to disease symptoms (≥20% weight loss). As expected, cells recovered from off-dox recipient mice showed major downregulation of IL-7Rα to levels comparable to DP cells of F5 control mice, which express low to undetectable levels of IL-7Rα (**Fig. 3A**). However, the leukemia cells presented a similar immunophenotype (**Fig. 3B**) and were found in similar numbers to those recovered from dox fed hosts. These results

suggest that, at least in some cases, high levels of wild type IL-7Rα expression may be redundant for the maintenance of fully established leukemias once transformation has occurred.

TetIL-7R tumors display hyperactivation of PI3K/Akt pathway and mimic multiple features of human T-ALL

Remarkably, Tet-IL-7R tumors mimicked numerous important features of human T-ALL. First, their immunophenotype varied considerably between animals (from CD4 CD8 double-negative to double positive to CD4 or CD8 single positive cells), reflecting the different stages of maturation block known to occur in the human disease (**Fig. 1C**) [46,47]. Second, heterogeneity extended to the genetic subset of T-ALL affecting each animal. Transcriptomics analyses showed that tumors resemble different major human T-ALL subsets [31], tending to cluster into two main groups (TAL/LMO+Proliferative or HOXA/TLX+immature; **Fig. 4A**). Taken together, these results suggest that IL-7R-mediated transformation is not restricted to a particular T-ALL oncogenetic subtype, in agreement to what appears to happen with mutant *IL7R* in human T-ALL [6,12], or to a single maturation stage, in accordance with the fact that human T-ALL cells respond to IL-7 irrespectively of their stage of differentiation [19].

Third, similar to the majority of primary T-ALL cases, most tumors displayed hyperactivation of PI3K/Akt pathway [45,46,48], sometimes associated with absence or decreased Pten protein expression (**Fig. 4B**) and *Pten* mutation (**Table S1**). In agreement, gene set enrichment analysis (GSEA) of differentially expressed genes between tumors and controls revealed a strong enrichment for phosphadidylinositol and mTOR (**Fig. 4C**, **Fig. 4D**) signaling in tumors. Fourth, in accordance with increased IL-7R-mediated signaling, and similar to human T-ALL [6,23,24,49-53], the tumors were enriched in genes upregulated in JAK/STAT pathway signaling (**Fig. 4E**). Fifth, we found evidence of *Notch1* mutation (**Table S1**) and Notch signaling activation (**Fig. 4F**), a hallmark of both mouse and human T-ALL. Sixth, in accordance with increased proliferation (**Fig. 1C and 4G**), the cell cycle inhibitor $p27^{Kip1}$ was frequently downregulated (**Fig. 4B**), a molecular

characteristic of human T-ALL cells [54], and particularly of IL-7-responsive cases [16,21]. Finally, the expression of Bcl-2, which is upregulated by and mandatory for IL-7-mediated viability of primary human T-ALL cells [15-17], was also higher in the tumors (**Fig. 4H**).

Human IL-7Rα expression leads to the dose-dependent development of T-cell leukemias that are sensitive to inhibition of different IL-7R downstream effectors

Next, we evaluated whether the human wild type IL-7Rα had a similar oncogenic potential to the mouse and assessed if higher levels of receptor expression are more efficient in driving T-cell malignancy. To do this, we modified the ubiquitously expressed *Rosa26* locus to express human *IL7R*. LoxP flanked TpA stop signals prevented constitutive *IL7R* gene expression. However, introducing a huCD2-Cre transgene generated mice in which human IL-7Rα expression was released in lymphoid precursors (Rosa26-hIL-7R.huCD2-Cre hereafter referred to as R26-hIL-7R) developing in an otherwise normal immune background. As expected, homozygous mice (hIL-7R+/+), with two copies of *hIL7R*, displayed higher surface hIL-7Rα levels than heterozygous (hIL-7R+/-) mice (**Fig. 5A, B**), whereas expression of other γc family cytokine receptors was not affected by IL-7R overexpression (**Fig. S5**). Notably, hIL-7R+/+ animals also developed malignant disease significantly faster than hIL-7R+/- (**Fig. 5C**), indicating an IL-7Rα dose-dependent leukemogenic effect. Analysis of hIL-7R+/+ mice with disease revealed expansion of CD8+CD4-TCR^{lo} thymocytes (**Fig. 5D**) with a proliferative phenotype (**Fig. 5E**) and an increased thymic size (**Fig. 5F**). Malignant T cells spread to the bone marrow (**Fig. 5D, E**) and spleen (**Fig. 5D-F**), presenting with splenomegaly (**Fig. 5F**). Full necropsy showed also leukemia spread to lymph nodes, heart, lung, liver, kidney, and central nervous system (**Fig. S6A**). Flow cytometry analysis did not reveal any B-cell malignancies, all leukemias being CD19 negative and displaying only T cell markers (**Fig. S6B**). Transplant experiments into *Rag1*$^{-/-}$ *Il2rg*$^{-/-}$ versus *Rag1*$^{-/-}$ *Il2rg*$^{-/-}$ *Il7*$^{-/-}$ mice showed that established tumors remained IL-7-responsive, although leukemia/lymphoma was

eventually propagated even in the absence of IL-7 (**Fig. 5G**). These results were in line with those from the dox-inducible model and indicated that full-blown leukemias triggered by high levels of IL-7R expression were no longer necessarily fully reliant on microenvironmental IL-7-mediated signals for their propagation.

To examine putative mechanisms justifying these observations and identify secondary hits collaborating with high IL-7R expression in driving T-ALL, we performed whole exome sequencing (WES) of leukemia samples from R26-hIL-7R mice. As expected, *Notch1*, a major T-ALL oncogene, was frequently mutated (**Fig 5H** and **Table S2**). In addition, we found mutations in *Rb1*, *Atrx*, *Ptchd4* and *Idh1*, which are known cancer drivers, including in T-ALL. Other affected genes included *Fat3* (belonging to the same functional family as the T-ALL driver *Fat1*), *Csfr3* (which is mutated in myeloid leukemias), and *Klf13* (involved in B and T-cell development). Notably, some of the tumors displayed mutations in genes that are directly related to IL-7R downstream signaling, such as *Ptprc* (CD45), whose loss-of-function mutation in T-ALL potentiates JAK/STAT signaling [55], *Ago2*, which interplays with KRAS signaling [56], and *Asns*, known to be upregulated by IL-7R signaling [57] (**Fig. 5H** and **Table S2**). In addition, although IL-7 levels were not significantly different between IL-7R-overexpressing mice and controls, as measured by qPCR in lymph nodes and ELISA in the blood **(Fig. S7)**, we found that some of the tumors displayed detectable IL-7 transcript levels (**Fig. 5I**), suggesting that, similar to human T-ALL [58], some mouse leukemias may display IL-7 autocrine production.

Irrespectively of the mechanism, leukemias arising from hIL-7R overexpression displayed IL-7R signaling activation, as assessed by Bcl-2 upregulation (**Fig. 5J**). Accordingly, the Bcl-2 inhibitor Venetoclax triggered leukemia cell death and prevented IL-7-mediated viability in a dose-dependent manner (**Fig. 5K**). Similar results were obtained with inhibitors of other IL-7R effectors, such as JAK1 [24,52,59], PI3K/mTOR [21,22], PIM1 [23,60], or Cdk4/6 [16], which also had cytotoxic effects on T-ALL cells (**Fig. S8**). Taken together, these observations suggest that acquisition of second

hits leading to activation of downstream IL-7R signaling may be the reason why some cases are no longer fully dependent on microenvironmental IL-7 or require high IL-7R surface expression and yet still display clear evidence of IL-7/IL-7R downstream activation.

T-ALL patients with high wild type *IL7R* expression display evidence of oncogenic IL-7R-dependent signaling activation

To further confirm the relevance of our findings for human disease, we next analyzed *IL7R* expression in a cohort of *IL7R* wild type T-ALL cases. We found highly heterogeneous expression of *IL7R* (**Fig. 6A**). We then compared the 20 cases with highest versus the 20 cases with lowest *IL7R* expression and gene set enrichment analysis of differentially expressed genes showed enrichment of genes that are targets of IL-7 stimulation[61] (NES=2.044, p<0.001) in the *IL7R*-high samples. These data demonstrate that human T-ALL cases with high levels of wild type *IL7R* display evidence for active IL-7 receptor signaling (**Fig. 6B**). Importantly, genes upregulated in *IL7R* mutant T-ALL samples were also enriched in wild type *IL7R*-high cases (NES=1.635, p=0.01), whereas genes downregulated in *IL7R* mutant cases showed negative enrichment (NES=-1.277, p=0.0069; **Fig. 6C**). These results indicate that high levels of expression of wild type IL-7Rα in human T-ALL patients are associated with a gene expression signature that resembles that of *IL7R* mutant cases.

Discussion

IL7R mutational activation is a known driver of T-ALL [6-13]. In addition, several mechanisms can lead to increased expression of wild type IL-7Rα in T-ALL, namely Notch activation [62], RPL10 R98S mutation [63] or ZEB2 translocation [64]. Mutations in genes such as DNM2 [65], which regulate IL-7Rα trafficking and surface availability [66], also potentially contribute to oncogenic IL-7R-mediated signaling. Most notably, there are reported cases of *IL7R* gene

amplification in T-ALL [26,27]. However, whether high IL-7Rα levels can drive T-ALL remains unaddressed. Whereas correlative evidence associates expression of IL-7Rα in AKR/J mice with leukemia development [67], and recent studies showed a correlation between high levels of IL-7R expression and increased leukemia stem cell activity in established human T-ALL [68], there is no direct proof of the oncogenic potential of overexpression of IL-7Rα without gain-of-function mutation. This is of clinical relevance, since there is a significant fraction of T-ALL patients that present with very high *IL7R* levels and, as we demonstrated here, gene expression profiling indicates that the leukemia cells display evidence for ongoing IL-7/IL-7R signaling activation that resembles that of oncogenic *IL7R* mutant T-ALL cases. Deep characterization of the similarities and differences between mutant and high-level wild type IL-7R signaling and downstream gene expression changes may expose therapeutic vulnerabilities and merits investigation. Our analyses of patient data suggest that not only mutational activation of IL-7Rα but also high levels of expression may be oncogenic. We confirmed this possibility by providing clear evidence, using two different *in vivo* models, that IL-7Rα is oncogenic even in the absence of mutational activation. Again, this is clinically relevant, because it implicates that also T-ALL cases with high IL-7Rα expression may benefit from treatment with inhibitors of IL7R-mediated signaling, including JAK1/3, PIM1, PI3K and IL-7R itself [25,69,70]. Anti-IL-7Rα antibodies are promising new therapeutic tools against T-ALL [69,70] and their impact particularly on *IL7R* high T-ALL cases warrants investigation. However, our findings indicating that some mouse T-ALLs no longer require high levels of IL-7R expression for leukemia maintenance serve as an alert that targeting of the receptor may not always be effective therapeutically. This may be because of genetic lesions on *Notch1*, *Atrx*, *Ptchd4* or *Idh1*, which could drive a shift in oncogene addiction, or it may be because of the acquisition of mutations such as those we found in *Ptprc*, *Ago2*, *Asns*, *Pten* or *Rb1*, which are either regulated by, or interplay with, signaling pathways activated by IL-7R and thus can mimic or lead to IL-7R-mediated downstream signaling activation. In agreement with the latter,

leukemia samples remain sensitive to pharmacological inhibitors of IL-7R signaling effectors, such as JAK1 (Ruxolitinib), PI3K/mTOR (Dactolisib) or PIM1 (AZD1208) [6,21-24,27,52,59,60].

Our studies also suggest that IL-7Rα overexpression may promote thymocyte self-renewal by 8 weeks of age, in a majority of the cases, eventually leading to subsequent leukemia development. An alternative (not mutually exclusive) explanation as to why some of the cases display a (pre)leukemic phenotype would be the acquisition of secondary oncogenic hits, which would not necessarily involve previous engagement of a self-renewal program. Further experiments are warranted to determine more exactly for how long is high expression of IL-7R required to consistently engage self-renewal and/or a leukemogenic program.

The mouse tumors that develop downstream from IL-7Rα mimic multiple features of human T-ALL, including interpatient heterogeneity in immunophenotype and oncogenetic subtype, similar to what was found for cases with *IL7R* mutation, which occur in different T-ALL subtypes [12]. Our *in vivo* models may therefore be instrumental for the thorough characterization of IL-7R-mediated T-ALL, the potential unmasking of molecular targets for therapeutic intervention and the testing of novel treatment strategies. Obvious candidates for therapeutic intervention include, as stated above, inhibitors of JAK/STAT/PIM pathway or PI3K/Akt signaling [21-24,27,52,60,71], whose efficacy we also demonstrated here by the use of Ruxolitinib, AZD1208 and Dactolisib in IL-7R-overexpressing mouse leukemias. Given the known positive impact of IL-7/IL-7R-mediated signaling on Bcl-2 expression in T-ALL cells [16,17,21,23,72], we also tested the BH3 mimetic drug Venetoclax, which clearly promoted cell death *in vitro*. These results are in line with other studies providing evidence for the potential of Bcl-2 inhibitors against T-ALL [73-75]. Additionally, in agreement with IL-7 inducing cell cycle progression in human T-ALL cells [16], we demonstrated the efficacy of the Cdk4/6 inhibitor Palbociclib [76] in our mouse T-ALLs.

Overall, our studies provide the first direct evidence that IL-7Rα can promote T-cell tumorigenesis in a dose-dependent manner, even in the absence of *IL7R* gain-of-function

mutations. Our findings are of particular relevance for the understanding of the biology and the treatment of T-ALL cases with high *IL7R* levels, including those with *IL7R* gains.

Acknowledgements

We thank S. Tung and MRC National Institute for Medical Research Biological Services staff for assistance with mouse breeding and typing. We are also grateful to the Medical Research Council (MRC) National Institute for Medical Research flow cytometry and high-throughput sequencing core facilities, as well as to Pedro Ruivo and iMM's Comparative Pathology Unit. We further acknowledge Marta Fernandes for preparing the visual abstract. The work was supported by the MRC (United Kingdom) under Programme Codes U117573801 and MR/P011225/1, to BS; and by the consolidator grant ERC CoG-648455 from the European Research Council, under the European Union's Horizon 2020 research and innovation programme, and the FAPESP/20015/2014 grant from FCT, to JTB. AS received a fellowship from FCT (SFRH/BD/18388/2004). JTB was an FCT Investigator (consolidator) and ARG the recipient of an FCT Investigator grant (IF/00510/2014). This work was also supported by a grant from the foundation "Fonds Kinderen Kankervrij" (KiKa 2010-082; YL).

Authorship contributions

AS and AA designed and performed experiments, analyzed and interpreted data; AC and TH performed experiments; JLN, MM, SD and YL conducted bioinformatics analyses; JM, JC and ARG supervised the bioinformatics analyses and provided critical suggestions and feedback; BS and JTB designed research, analyzed and interpreted data, supervised the studies and wrote the manuscript. All authors critically read and contributed to the final version of the manuscript.

Conflict of interest disclosures

The authors declare no conflict of interest.

References

1. Fry TJ, Mackall CL. Interleukin-7: from bench to clinic. *Blood*. 2002;99(11):3892-3904.
2. Peschon JJ, Morrissey PJ, Grabstein KH, et al. Early lymphocyte expansion is severely impaired in interleukin 7 receptor-deficient mice. *J Exp Med*. 1994;180(5):1955-1960.
3. von Freeden-Jeffry U, Vieira P, Lucian LA, McNeil T, Burdach SE, Murray R. Lymphopenia in interleukin (IL)-7 gene-deleted mice identifies IL-7 as a nonredundant cytokine. *J Exp Med*. 1995;181(4):1519-1526.
4. Barata JT, Durum SK, Seddon B. Flip the coin: IL-7 and IL-7R in health and disease. *Nat Immunol*. 2019;20(12):1584-1593.
5. Puel A, Ziegler SF, Buckley RH, Leonard WJ. Defective IL7R expression in T(-)B(+)NK(+) severe combined immunodeficiency. *Nat Genet*. 1998;20(4):394-397.
6. Zenatti PP, Ribeiro D, Li W, et al. Oncogenic IL7R gain-of-function mutations in childhood T-cell acute lymphoblastic leukemia. *Nat Genet*. 2011;43(10):932-939.
7. Shochat C, Tal N, Bandapalli OR, et al. Gain-of-function mutations in interleukin-7 receptor-{alpha} (IL7R) in childhood acute lymphoblastic leukemias. *J Exp Med*. 2011;208(5):901-908.
8. Zhang J, Ding L, Holmfeldt L, et al. The genetic basis of early T-cell precursor acute lymphoblastic leukaemia. *Nature*. 2012;481(7380):157-163.
9. Treanor LM, Zhou S, Janke L, et al. Interleukin-7 receptor mutants initiate early T cell precursor leukemia in murine thymocyte progenitors with multipotent potential. *J Exp Med*. 2014;211(4):701-713.
10. Yokoyama K, Yokoyama N, Izawa K, et al. In vivo leukemogenic potential of an interleukin 7 receptor alpha chain mutant in hematopoietic stem and progenitor cells. *Blood*. 2013;122(26):4259-4263.
11. De Keersmaecker K, Atak ZK, Li N, et al. Exome sequencing identifies mutation in CNOT3 and ribosomal genes RPL5 and RPL10 in T-cell acute lymphoblastic leukemia. *Nat Genet*. 2013;45(2):186-190.
12. Liu Y, Easton J, Shao Y, et al. The genomic landscape of pediatric and young adult T-lineage acute lymphoblastic leukemia. *Nat Genet*. 2017;49(8):1211-1218.
13. Cante-Barrett K, Spijkers-Hagelstein JA, Buijs-Gladdines JG, et al. MEK and PI3K-AKT inhibitors synergistically block activated IL7 receptor signaling in T-cell acute lymphoblastic leukemia. *Leukemia*. 2016;30(9):1832-1843.
14. Rich BE, Campos-Torres J, Tepper RI, Moreadith RW, Leder P. Cutaneous lymphoproliferation and lymphomas in interleukin 7 transgenic mice. *J Exp Med*. 1993;177(2):305-316.
15. Silva A, Laranjeira AB, Martins LR, et al. IL-7 contributes to the progression of human T-cell acute lymphoblastic leukemias. *Cancer Res*. 2011;71(14):4780-4789.
16. Barata JT, Cardoso AA, Nadler LM, Boussiotis VA. Interleukin-7 promotes survival and cell cycle progression of T-cell acute lymphoblastic leukemia cells by down-regulating the cyclin-dependent kinase inhibitor p27(kip1). *Blood*. 2001;98(5):1524-1531.
17. Karawajew L, Ruppert V, Wuchter C, et al. Inhibition of in vitro spontaneous apoptosis by IL-7 correlates with bcl-2 up-regulation, cortical/mature immunophenotype, and better early cytoreduction of childhood T-cell acute lymphoblastic leukemia. *Blood*. 2000;96(1):297-306.
18. Scupoli MT, Perbellini O, Krampera M, Vinante F, Cioffi F, Pizzolo G. Interleukin 7 requirement for survival of T-cell acute lymphoblastic leukemia and human thymocytes on bone marrow stroma. *Haematologica*. 2007;92(2):264-266.
19. Barata JT, Keenan TD, Silva A, Nadler LM, Boussiotis VA, Cardoso AA. Common gamma chain-signaling cytokines promote proliferation of T-cell acute lymphoblastic leukemia. *Haematologica*. 2004;89(12):1459-1467.

20. Dibirdik I, Langlie MC, Ledbetter JA, et al. Engagement of interleukin-7 receptor stimulates tyrosine phosphorylation, phosphoinositide turnover, and clonal proliferation of human T-lineage acute lymphoblastic leukemia cells. *Blood*. 1991;78(3):564-570.
21. Barata JT, Silva A, Brandao JG, Nadler LM, Cardoso AA, Boussiotis VA. Activation of PI3K Is Indispensable for Interleukin 7-mediated Viability, Proliferation, Glucose Use, and Growth of T Cell Acute Lymphoblastic Leukemia Cells. *J Exp Med*. 2004;200(5):659-669.
22. Silva A, Girio A, Cebola I, Santos CI, Antunes F, Barata JT. Intracellular reactive oxygen species are essential for PI3K/Akt/mTOR-dependent IL-7-mediated viability of T-cell acute lymphoblastic leukemia cells. *Leukemia*. 2011;25(6):960-967.
23. Ribeiro D, Melao A, van Boxtel R, et al. STAT5 is essential for IL-7-mediated viability, growth, and proliferation of T-cell acute lymphoblastic leukemia cells. *Blood Adv*. 2018;2(17):2199-2213.
24. Delgado-Martin C, Meyer LK, Huang BJ, et al. JAK/STAT pathway inhibition overcomes IL7-induced glucocorticoid resistance in a subset of human T-cell acute lymphoblastic leukemias. *Leukemia*. 2017;31(12):2568-2576.
25. Cramer SD, Aplan PD, Durum SK. Therapeutic targeting of IL-7Ralpha signaling pathways in ALL treatment. *Blood*. 2016;128(4):473-478.
26. Vicente C, Schwab C, Broux M, et al. Targeted sequencing identifies associations between IL7R-JAK mutations and epigenetic modulators in T-cell acute lymphoblastic leukemia. *Haematologica*. 2015;100(10):1301-1310.
27. Li Y, Buijs-Gladdines JG, Cante-Barrett K, et al. IL-7 Receptor Mutations and Steroid Resistance in Pediatric T cell Acute Lymphoblastic Leukemia: A Genome Sequencing Study. *PLoS Med*. 2016;13(12):e1002200.
28. Buentke E, Mathiot A, Tolaini M, Di Santo J, Zamoyska R, Seddon B. Do CD8 effector cells need IL-7R expression to become resting memory cells? *Blood*. 2006;108(6):1949-1956.
29. de Boer J, Williams A, Skavdis G, et al. Transgenic mice with hematopoietic and lymphoid specific expression of Cre. *Eur J Immunol*. 2003;33(2):314-325.
30. Grabherr MG, Haas BJ, Yassour M, et al. Full-length transcriptome assembly from RNA-Seq data without a reference genome. *Nat Biotechnol*. 2011;29(7):644-652.
31. Homminga I, Pieters R, Langerak A, et al. Integrated transcript and genome analyses reveal NKX2-1 and MEF2C as potential oncogenes in T -cell acute lymphoblastic leukemia. *Cancer Cell*. 2011;19(4):484-497.
32. Gautier L, Cope L, Bolstad BM, Irizarry RA. affy--analysis of Affymetrix GeneChip data at the probe level. *Bioinformatics*. 2004;20(3):307-315.
33. Durinck S, Spellman PT, Birney E, Huber W. Mapping identifiers for the integration of genomic datasets with the R/Bioconductor package biomaRt. *Nat Protoc*. 2009;4(8):1184-1191.
34. Subramanian A, Tamayo P, Mootha VK, et al. Gene set enrichment analysis: a knowledge-based approach for interpreting genome-wide expression profiles. *Proc Natl Acad Sci U S A*. 2005;102(43):15545-15550.
35. Ritchie ME, Phipson B, Wu D, et al. limma powers differential expression analyses for RNA-sequencing and microarray studies. *Nucleic Acids Res*. 2015;43(7):e47.
36. Boudil A, Matei IR, Shih HY, et al. IL-7 coordinates proliferation, differentiation and Tcra recombination during thymocyte beta-selection. *Nat Immunol*. 2015;16(4):397-405.
37. Degryse S, de Bock CE, Cox L, et al. JAK3 mutants transform hematopoietic cells through JAK1 activation, causing T-cell acute lymphoblastic leukemia in a mouse model. *Blood*. 2014;124(20):3092-3100.
38. Chaudhry MS, Velardi E, Dudakov JA, van den Brink MR. Thymus: the next (re)generation. *Immunol Rev*. 2016;271(1):56-71.
39. Chinn IK, Blackburn CC, Manley NR, Sempowski GD. Changes in primary lymphoid organs with aging. *Semin Immunol*. 2012;24(5):309-320.

40. Larson RC, Lavenir I, Larson TA, et al. Protein dimerization between Lmo2 (Rbtn2) and Tal1 alters thymocyte development and potentiates T cell tumorigenesis in transgenic mice. *Embo J*. 1996;15(5):1021-1027.
41. O'Neil J, Shank J, Cusson N, Murre C, Kelliher M. TAL1/SCL induces leukemia by inhibiting the transcriptional activity of E47/HEB. *Cancer Cell*. 2004;5(6):587-596.
42. Trinquand A, Dos Santos NR, Tran Quang C, et al. Triggering the TCR Developmental Checkpoint Activates a Therapeutically Targetable Tumor Suppressive Pathway in T-cell Leukemia. *Cancer Discov*. 2016;6(9):972-985.
43. Bessette K, Lang ML, Fava RA, et al. A Stat5b transgene is capable of inducing CD8+ lymphoblastic lymphoma in the absence of normal TCR/MHC signaling. *Blood*. 2008;111(1):344-350.
44. Papaemmanuil E, Rapado I, Li Y, et al. RAG-mediated recombination is the predominant driver of oncogenic rearrangement in ETV6-RUNX1 acute lymphoblastic leukemia. *Nat Genet*. 2014;46(2):116-125.
45. Mendes RD, Sarmento LM, Cante-Barrett K, et al. PTEN microdeletions in T-cell acute lymphoblastic leukemia are caused by illegitimate RAG-mediated recombination events. *Blood*. 2014;124(4):567-578.
46. Silva A, Yunes JA, Cardoso BA, et al. PTEN posttranslational inactivation and hyperactivation of the PI3K/Akt pathway sustain primary T cell leukemia viability. *J Clin Invest*. 2008;118(11):3762-3774.
47. Ferrando AA, Neuberg DS, Staunton J, et al. Gene expression signatures define novel oncogenic pathways in T cell acute lymphoblastic leukemia. *Cancer Cell*. 2002;1(1):75-87.
48. Gutierrez A, Sanda T, Grebliunaite R, et al. High frequency of PTEN, PI3K, and AKT abnormalities in T-cell acute lymphoblastic leukemia. *Blood*. 2009;114(3):647-650.
49. Flex E, Petrangeli V, Stella L, et al. Somatically acquired JAK1 mutations in adult acute lymphoblastic leukemia. *J Exp Med*. 2008;205(4):751-758.
50. Kontro M, Kuusanmaki H, Eldfors S, et al. Novel activating STAT5B mutations as putative drivers of T-cell acute lymphoblastic leukemia. *Leukemia*. 2014;28(8):1738-1742.
51. Bandapalli OR, Schuessele S, Kunz JB, et al. The activating STAT5B N642H mutation is a common abnormality in pediatric T-cell acute lymphoblastic leukemia and confers a higher risk of relapse. *Haematologica*. 2014;99(10):e188-192.
52. Maude SL, Dolai S, Delgado-Martin C, et al. Efficacy of JAK/STAT pathway inhibition in murine xenograft models of early T-cell precursor (ETP) acute lymphoblastic leukemia. *Blood*. 2015;125(11):1759-1767.
53. Degryse S, Bornschein S, de Bock CE, et al. Mutant JAK3 signaling is increased by loss of wild-type JAK3 or by acquisition of secondary JAK3 mutations in T-ALL. *Blood*. 2018;131(4):421-425.
54. Wolfraim LA, Fernandez TM, Mamura M, et al. Loss of Smad3 in acute T-cell lymphoblastic leukemia. *N Engl J Med*. 2004;351(6):552-559.
55. Porcu M, Kleppe M, Gianfelici V, et al. Mutation of the receptor tyrosine phosphatase PTPRC (CD45) in T-cell acute lymphoblastic leukemia. *Blood*. 2012;119(19):4476-4479.
56. Shankar S, Pitchiaya S, Malik R, et al. KRAS Engages AGO2 to Enhance Cellular Transformation. *Cell Rep*. 2016;14(6):1448-1461.
57. Zeng H, Yu M, Tan H, et al. Discrete roles and bifurcation of PTEN signaling and mTORC1-mediated anabolic metabolism underlie IL-7-driven B lymphopoiesis. *Sci Adv*. 2018;4(1):eaar5701.
58. Buffiere A, Uzan B, Aucagne R, et al. T-cell acute lymphoblastic leukemia displays autocrine production of Interleukin-7. *Oncogene*. 2019;38(48):7357-7365.

59. Melao A, Spit M, Cardoso BA, Barata JT. Optimal interleukin-7 receptor-mediated signaling, cell cycle progression and viability of T-cell acute lymphoblastic leukemia cells rely on casein kinase 2 activity. *Haematologica*. 2016;101(11):1368-1379.
60. De Smedt R, Morscio J, Reunes L, et al. Targeting cytokine- and therapy-induced PIM1 activation in preclinical models of T-cell acute lymphoblastic leukemia and lymphoma. *Blood*. 2020;135(19):1685-1695.
61. Bornschein S, Demeyer S, Stirparo R, et al. Defining the molecular basis of oncogenic cooperation between TAL1 expression and Pten deletion in T-ALL using a novel pro-T-cell model system. *Leukemia*. 2018;32(4):941-951.
62. Gonzalez-Garcia S, Garcia-Peydro M, Martin-Gayo E, et al. CSL-MAML-dependent Notch1 signaling controls T lineage-specific IL-7R{alpha} gene expression in early human thymopoiesis and leukemia. *J Exp Med*. 2009;206(4):779-791.
63. Girardi T, Vereecke S, Sulima SO, et al. The T-cell leukemia-associated ribosomal RPL10 R98S mutation enhances JAK-STAT signaling. *Leukemia*. 2017.
64. Goossens S, Radaelli E, Blanchet O, et al. ZEB2 drives immature T-cell lymphoblastic leukaemia development via enhanced tumour-initiating potential and IL-7 receptor signalling. *Nat Commun*. 2015;6:5794.
65. Tremblay CS, Brown FC, Collett M, et al. Loss-of-function mutations of Dynamin 2 promote T-ALL by enhancing IL-7 signalling. *Leukemia*. 2016;30(10):1993-2001.
66. Tremblay CS, Chiu SK, Saw J, et al. Small molecule inhibition of Dynamin-dependent endocytosis targets multiple niche signals and impairs leukemia stem cells. *Nat Commun*. 2020;11(1):6211.
67. Laouar Y, Crispe IN, Flavell RA. Overexpression of IL-7R alpha provides a competitive advantage during early T-cell development. *Blood*. 2004;103(6):1985-1994.
68. Gonzalez-Garcia S, Mosquera M, Fuentes P, et al. IL-7R is essential for leukemia-initiating cell activity of T-cell acute lymphoblastic leukemia. *Blood*. 2019;134(24):2171-2182.
69. Akkapeddi P, Fragoso R, Hixon JA, et al. A fully human anti-IL-7Ralpha antibody promotes antitumor activity against T-cell acute lymphoblastic leukemia. *Leukemia*. 2019;33(9):2155-2168.
70. Hixon JA, Andrews C, Kashi L, et al. New anti-IL-7Ralpha monoclonal antibodies show efficacy against T cell acute lymphoblastic leukemia in pre-clinical models. *Leukemia*. 2020;34(1):35-49.
71. Ksionda O, Melton AA, Bache J, et al. RasGRP1 overexpression in T-ALL increases basal nucleotide exchange on Ras rendering the Ras/PI3K/Akt pathway responsive to protumorigenic cytokines. *Oncogene*. 2016;35(28):3658-3668.
72. Senkevitch E, Li W, Hixon JA, et al. Inhibiting Janus Kinase 1 and BCL-2 to treat T cell acute lymphoblastic leukemia with IL7-Ralpha mutations. *Oncotarget*. 2018;9(32):22605-22617.
73. Sanda T, Tyner JW, Gutierrez A, et al. TYK2-STAT1-BCL2 pathway dependence in T-cell acute lymphoblastic leukemia. *Cancer Discov*. 2013;3(5):564-577.
74. Peirs S, Matthijssens F, Goossens S, et al. ABT-199 mediated inhibition of BCL-2 as a novel therapeutic strategy in T-cell acute lymphoblastic leukemia. *Blood*. 2014;124(25):3738-3747.
75. Kampen KR, Sulima SO, Verbelen B, et al. The ribosomal RPL10 R98S mutation drives IRES-dependent BCL-2 translation in T-ALL. *Leukemia*. 2019;33(2):319-332.
76. Gary JM, Simmons JK, Xu J, et al. Hypomorphic mTOR Downregulates CDK6 and Delays Thymic Pre-T LBL Tumorigenesis. *Mol Cancer Ther*. 2020;19(10):2221-2232.

Figure Legends

Figure 1. IL-7Rα expression results in progressive thymic hyperplasia and disseminated, fatal T-cell leukemia/lymphoma. (A) Scatter plot is of thymus cellularity *vs* age from WT control (WT, grey diamonds), F5 control (F5 Ctrl, open circles) and F5 TetIL-7R^{ON} mice (Red circles). Numbers indicate slope of line fit and 95% confidence intervals. **(B)** Density plots show CD4 *vs* CD8 expression by thymocytes and splenocytes from TetIL-7R^{ON} mice (n=36). Lymphoma/leukemia present in thymus and spleen were characterized by their expression of CD4 and CD8 into double negative (DN), CD8 single positive (CD8 SP), double positive (DP) and CD4 single positive (CD4 SP). A representative example of each phenotype is shown and the percent incidence of phenotype indicated under the phenotypic label. **(C)** Density plots show CD4 *vs* CD8 expression by thymocytes and splenocytes from TetIL-7R^{ON} or control C57Bl6/J mice. Histograms are of Ki67 labeling of thymocytes (top) and splenocytes (bottom) of the indicated subpopulation from either TetIL-7R^{ON} or C57Bl6/J control mice. **(D)** Line graph shows survival of cohorts of TetIL-7R^{ON} (n=8), *vs* TetIL-7R^{OFF} (n=4) and TreIL-7R+ rtTA– *Il7r*$^{-/-}$ mice (n=4). Mice were culled when they reached the defined humane endpoint (See Methods). p=0.0003. **(E)** Density plots show phenotype, in the indicated organs, of F5 TetIL-7R^{ON} mice identified with clinical signs of disease (tumor), as compared with IL-7R^{WT} F5 control mice (control). Density plots are of CD4 *vs* CD8 in the thymus, spleen and bone marrow of the indicated conditions. **(F)** Malignant thymocytes from donor mouse in (E) were transferred into *Rag1*$^{-/-}$ recipients (n=8). Four weeks later, thymus, spleen and bone marrow were analyzed for presence of donor cells. Data are the pool of two (D) or six (A-B) independent experiments, or representative of three (C, E-F) independent experiments.

Figure 2. Disease development is influenced by Rag1 expression but not TCR signaling. (A) Development of malignant disease was monitored in cohorts of TetIL-7R^{ON} mice, whose T cells

have a polyclonal TCR repertoire (Poly, n=8), and TCR transgenic F5 TetIL-7R^{ON} (F5, n=6) and OTII TetIL-7R^{ON} (OTII n=10) mice. Line graph shows survival of the different strains over time. **(B)** Survival of cohorts of F5 TetIL-7R^{ON} (Rag1+) and F5 *Rag1*$^{-/-}$ TetIL-7R^{ON} (n=11) mice was monitored up to 400 days of age. * p = 0.018; n.s., non-significant; Log-rank, Mantel-Cox test.

Figure 3. Maintenance of established TetIL-7R tumors no longer appears to require high IL-7Rα expression. (A) IL-7Rα expression was measured in F5 TetIL-7R primary tumor cells (left), and after adoptive transfer into *Rag1*$^{-/-}$ mice (right). Left: Mean fluorescence intensity (MFI) of primary tumor cells, collected from the thymus of a sick mouse continuously fed doxycycline (tumor), was compared to the DP (CD4+CD8+) population of an F5 control mouse (used as negative control). Right: Malignant cells collected from the thymus of the same mouse were transplanted into *Rag1*$^{-/-}$ recipient mice that were fed with (On dox) or without (Off dox) doxycycline-containing food for 4 weeks after transplant. MFI was compared after 4 weeks between On and Off dox groups. Graph: IL-7Rα MFI for each transplanted animal. **(B)** Transplanted cells collected from the bone marrow of On and Off dox recipient mice, 4 weeks after transplant, were compared for their immunophenotype. Top: density plot of CD4 *vs* CD8. Bottom: density plot of CD5 *vs* TCRαβ. Graphs: Frequency of cells within the gate represented on the left, for each transplanted animal. Results in the figure are representative of three independent experiments (from a different primary tumor each).

Figure 4. TetIL-7R tumors display hyperactivation of PI3K/Akt pathway and mimic multiple features of human T-ALL. (A) Hierarchical clustering analysis of Pearson correlation coefficients between mouse tumors and human T-ALL. Each row corresponds to a mouse leukemia and each lane to a human T-ALL sample. Transcriptomics analyses showed that mouse tumors resemble either TAL/LMO+Proliferative T-ALLs (cluster 1) or HOXA/TLX+immature (cluster 2), as

defined in Homminga et al [31]. Robustness of this analysis is shown by the fact that mouse leukemias that were 'classified' as HOXA/TLX+immature-like display features of immature/ETP-ALL, such as higher KIT, CD33 and CD34 than the other tumors, as shown in **Figure S4**. **(B)** Akt activation (p-Akt), and PTEN and $p27^{Kip1}$ expression levels were evaluated by immunoblot in on-dox F5 TetIL-7R thymic tumors (T-ALLs) versus control thymic samples from healthy, F5 mice (Ctrls). **(C-G)** Gene set enrichment analysis (GSEA) of the ranked expression differences between tumors and controls for the KEGG pathways: **(C)** phosphadidylinositol signaling, **(D)** mTOR signaling, **(E)** JAK-STAT signaling, **(F)** Notch signaling, and **(G)** cell cycle. **(H)** Bcl-2 expression levels were evaluated by immunoblot in tumors and controls.

Figure 5. Human IL-7Rα expression leads to the dose-dependent development of T-cell leukemias that are sensitive to Bcl-2 inhibition. (A) Flow cytometry analysis for hIL-7Rα within Lin^{neg} thymocytes from 12-week old animals of indicated genotypes. FMO, fluorescence minus one negative control. **(B)** Bar plot depicts difference to FMO of MFI of hIL-7Rα within each thymocyte subpopulation in heterozygous or homozygous animals. SD is indicated. **p<0.01; ***p<0.001; ****p<0.0001, Student's t-test. **(C)** Survival curves corresponding to the indicated genotypes. No leukemias were observed in the $CD2^{neg}$ hIL-$7R^{+/-}$ cohort (not shown). *p<0.05, Log-rank, Mantel-Cox test. $CD2^{neg}$ hIL-$7R^{+/+}$, n=23; $CD2^{pos}$ hIL-$7R^{+/-}$, n=28; $CD2^{pos}$ hIL$7R^{+/+}$, n=18. **(D-F)** Analysis of representative leukemic animal sacrificed when moribund. **(D)** Dot plots show CD4/CD8 coreceptor and CD8/TCRβ expression within Lin^{neg} thymocytes (Thy) and the presence of the same cells in the spleen (Spl) and bone marrow (BM). **(E)** CD8/Ki67 expression in Thy, Spl and BM. **(F)** Animal presented with a very large thymus and enlarged spleen. **(G)** Leukemic cells ($4x10^5$) were transferred into $Rag^{-/-}\gamma c^{-/-}$ or $Rag^{-/-}\gamma c^{-/-}$IL-$7^{-/-}$ hosts (n=8 each group) and survival curves are shown. (***p<0.001, Log-rank, Mantel-Cox). **(H)** Mutational burden map of SNVs and indel variants with predicted high and moderate impact in functionally relevant genes and drivers

of T-ALL or pediatric leukemias in $CD2^{pos}$ hIL-7R leukemias. **(I)** *Il7* mRNA expression levels relative to *hprt1* in leukemic cells from $CD2^{pos}$ hIL-7R leukemias were quantified by qRT-PCR. Average of triplicates and SD are shown. **(J)** Bcl-2 flow cytometry analysis of $CD4^{pos}TCR\beta^{pos}$ normal single positive thymocytes and $CD8^{pos}TCR\beta^{neg}$ leukemic cells of the same animal as in D-F. **(K)** Cells from two different leukemias (12895 and 14941) were cultured in the presence of the indicated doses of the Bcl-2 inhibitor Venetoclax and in the absence (red bars) or presence (purple bars) of IL-7. Bar plots and respective SD show viability at 48 hours. # $p<0.0001$, Venetoclax in the presence of IL-7 as compared to IL-7 alone; § $p<0.0001$, Venetoclax in the absence of IL-7 as compared to medium alone, One-Way ANOVA with Tukey's correction for multiple comparisons.

Figure 6. T-ALL patients with high wild type IL7R expression display evidence of oncogenic IL-7R-dependent signaling activation. **(A)** Normalized *IL7R* gene expression levels in T-ALL patients with wild type *IL7R* (n= 246). Dashed lines mark the 20 cases with highest expression (above top line) and the 20 cases with lowest *IL7R* expression (below bottom line), used for comparison in the subsequent analyses. Only *IL7R* wild type cases were analyzed. **(B-C)** Ranked GSEA on differentially expressed genes between *IL7R*-high and -low cases for the sets of **(B)** IL-7 target genes in pro-T cells, **(C)** genes upregulated in *IL7R* mutant T-ALL samples (left) and downregulated in *IL7R* mutant cases (right).

Figure 1

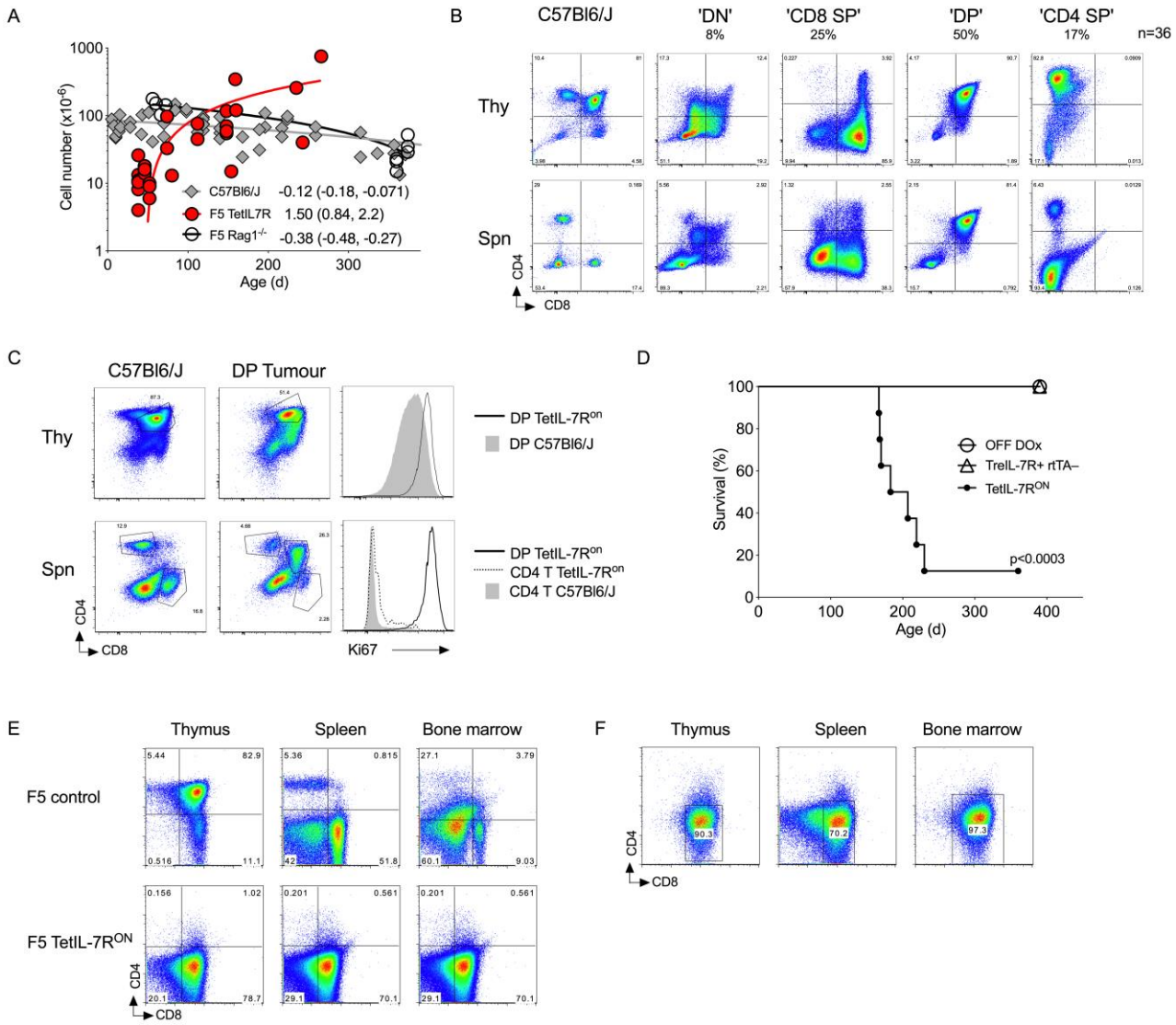
A
Cell number (x10^-6)
1000
100
10
1
0
100
200
300
Age (d)
C57Bl6/J -0.12 (-0.18, -0.071)
F5 TetIL7R 1.50 (0.84, 2.2)
F5 Rag1-/- -0.38 (-0.48, -0.27)
B
C57Bl6/J
'DN'
8%
'CD8 SP'
25%
'DP'
50%
'CD4 SP'
17%
n=36
Thy
Spn
CD4
CD8
C
C57Bl6/J
DP Tumour
Thy
Spn
CD4
CD8
Ki67
DP TetIL-7R^on
DP C57Bl6/J
DP TetIL-7R^on
CD4 T TetIL-7R^on
CD4 T C57Bl6/J
D
Survival (%)
100
80
60
40
20
0
0
100
200
300
400
Age (d)
OFF DOx
TreIL-7R+ rtTA–
TetIL-7R^ON
p<0.0003
E
Thymus
Spleen
Bone marrow
F5 control
F5 TetIL-7R^ON
CD4
CD8
F
Thymus
Spleen
Bone marrow
CD4
CD8

Figure 2

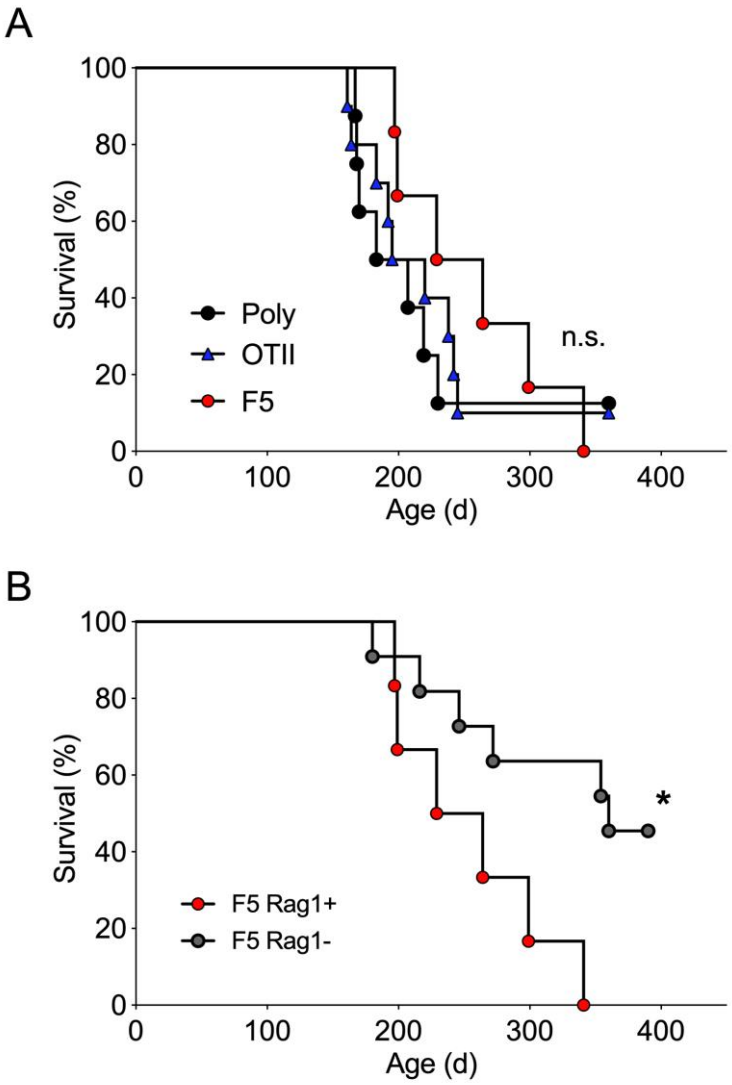
A
100
80
60
40
20
0
Survival (%)
Poly
OTII
F5
n.s.
0
100
200
300
400
Age (d)
B
100
80
60
40
20
0
Survival (%)
F5 Rag1+
F5 Rag1-
*
0
100
200
300
400
Age (d)

Figure 3

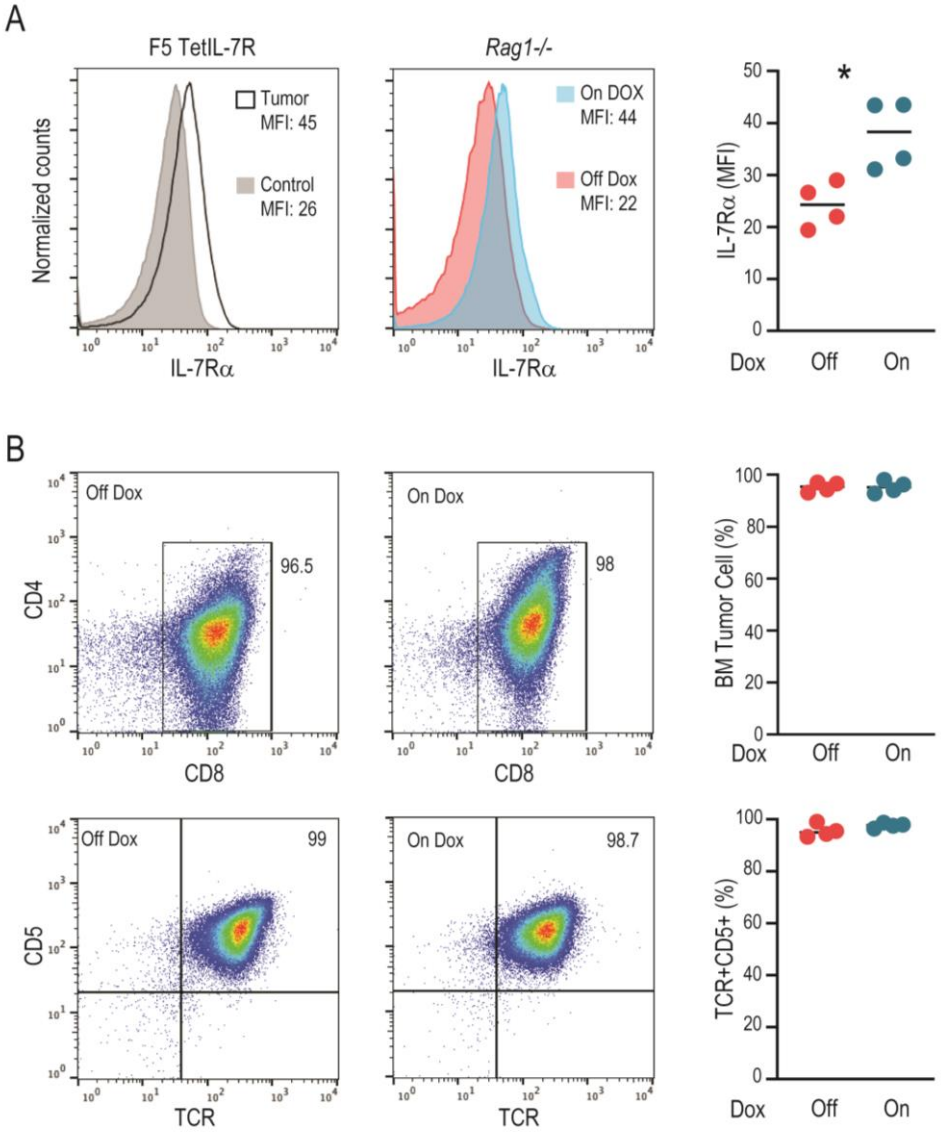
A
F5 TetIL-7R
Rag1-/-
Tumor
MFI: 45
Control
MFI: 26
On DOX
MFI: 44
Off Dox
MFI: 22
Normalized counts
IL-7Rα
IL-7Rα (MFI)
Dox
Off
On
B
Off Dox
On Dox
96.5
98
CD4
CD8
BM Tumor Cell (%)
99
98.7
CD5
TCR
TCR+CD5+ (%)

Figure 4

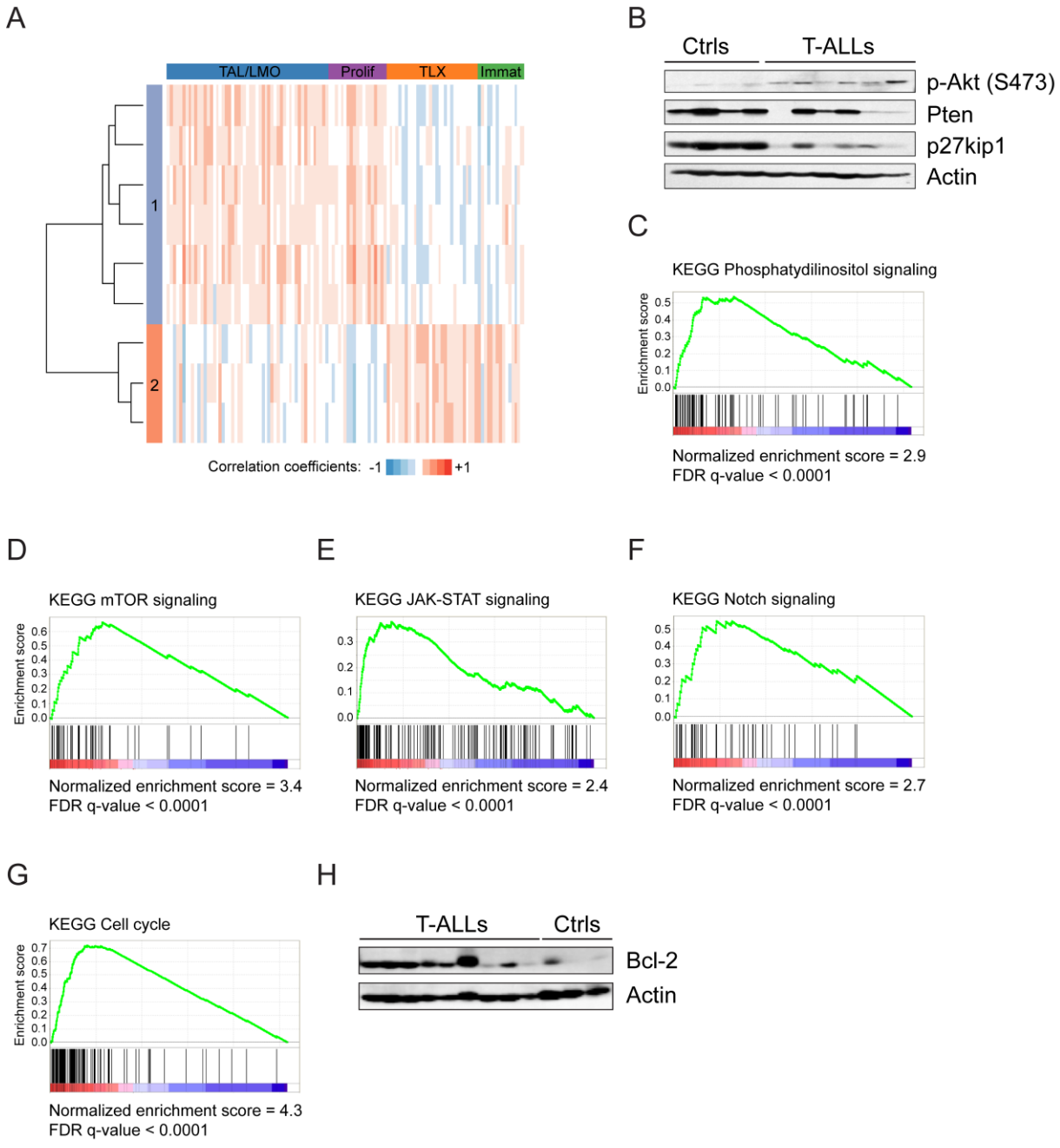
A
TAL/LMO
Prolif
TLX
Immat
1
2
Correlation coefficients: -1 +1
B
Ctrls
T-ALLs
p-Akt (S473)
Pten
p27kip1
Actin
C
KEGG Phosphatydilinositol signaling
Enrichment score
Normalized enrichment score = 2.9
FDR q-value < 0.0001
D
KEGG mTOR signaling
Enrichment score
Normalized enrichment score = 3.4
FDR q-value < 0.0001
E
KEGG JAK-STAT signaling
Normalized enrichment score = 2.4
FDR q-value < 0.0001
F
KEGG Notch signaling
Normalized enrichment score = 2.7
FDR q-value < 0.0001
G
KEGG Cell cycle
Enrichment score
Normalized enrichment score = 4.3
FDR q-value < 0.0001
H
T-ALLs
Ctrls
Bcl-2
Actin

Figure 5

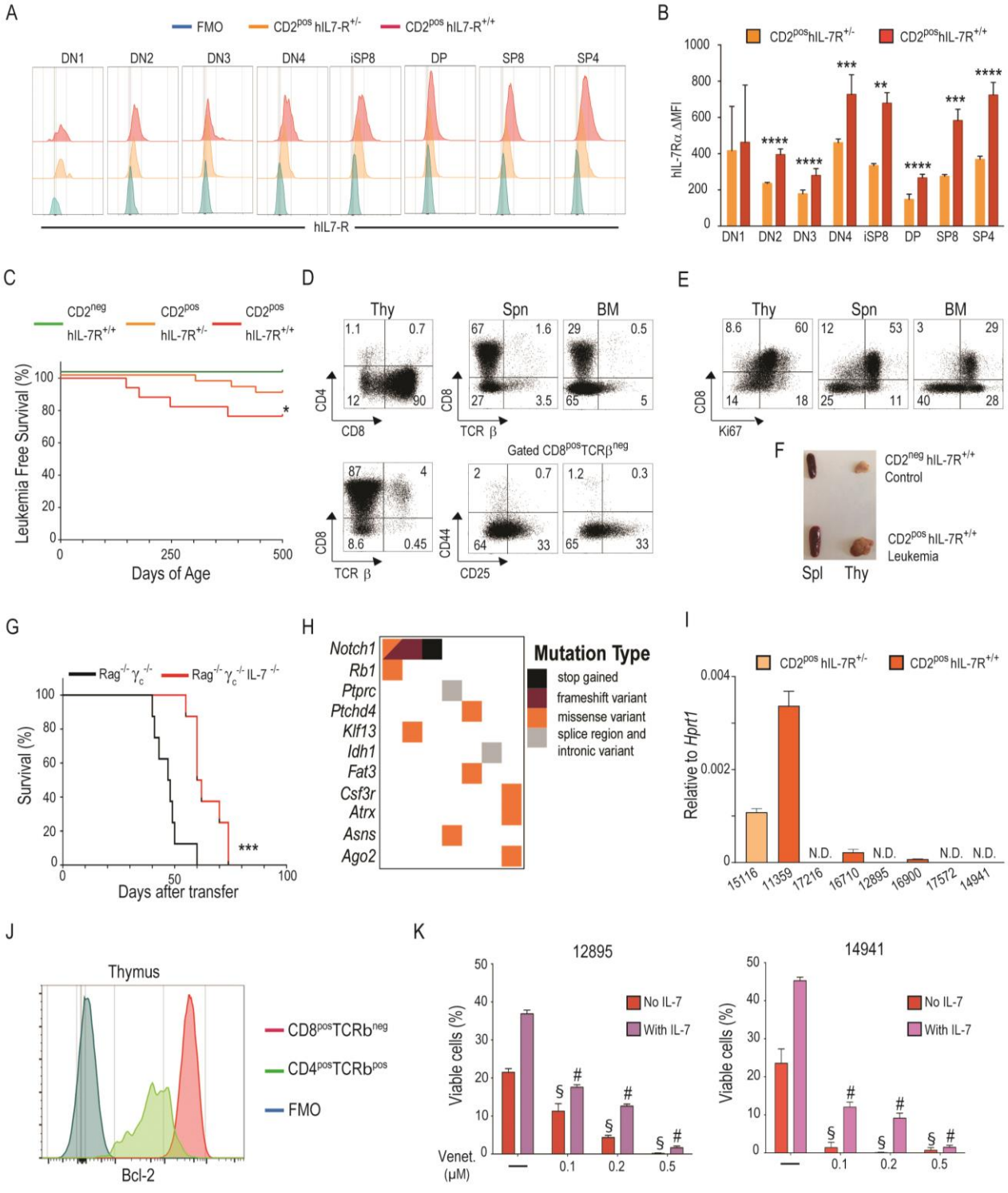
A
FMO
CD2pos hIL7-R+/-
CD2pos hIL7-R+/+
DN1
DN2
DN3
DN4
iSP8
DP
SP8
SP4
hIL7-R
B
CD2posIL-7R+/-
CD2posIL-7R+/+
hIL-7Rα ΔMFI
C
CD2neg hIL-7R+/+
CD2pos hIL-7R+/-
CD2pos hIL-7R+/+
Leukemia Free Survival (%)
Days of Age
D
Thy
Spn
BM
CD4
CD8
TCR β
Gated CD8posTCRβneg
CD44
CD25
E
Ki67
F
Control
Leukemia
Spl
Thy
G
Rag-/- γc-/-
Rag-/- γc-/- IL-7 -/-
Survival (%)
Days after transfer
H
Notch1
Rb1
Ptprc
Ptchd4
Klf13
Idh1
Fat3
Csf3r
Atrx
Asns
Ago2
Mutation Type
stop gained
frameshift variant
missense variant
splice region and intronic variant
I
Relative to Hprt1
N.D.
15116
11359
17216
16710
12895
16900
17572
14941
J
Thymus
CD8posTCRbneg
CD4posTCRbpos
FMO
Bcl-2
K
12895
14941
No IL-7
With IL-7
Viable cells (%)
Venet. (μM)

Figure 6

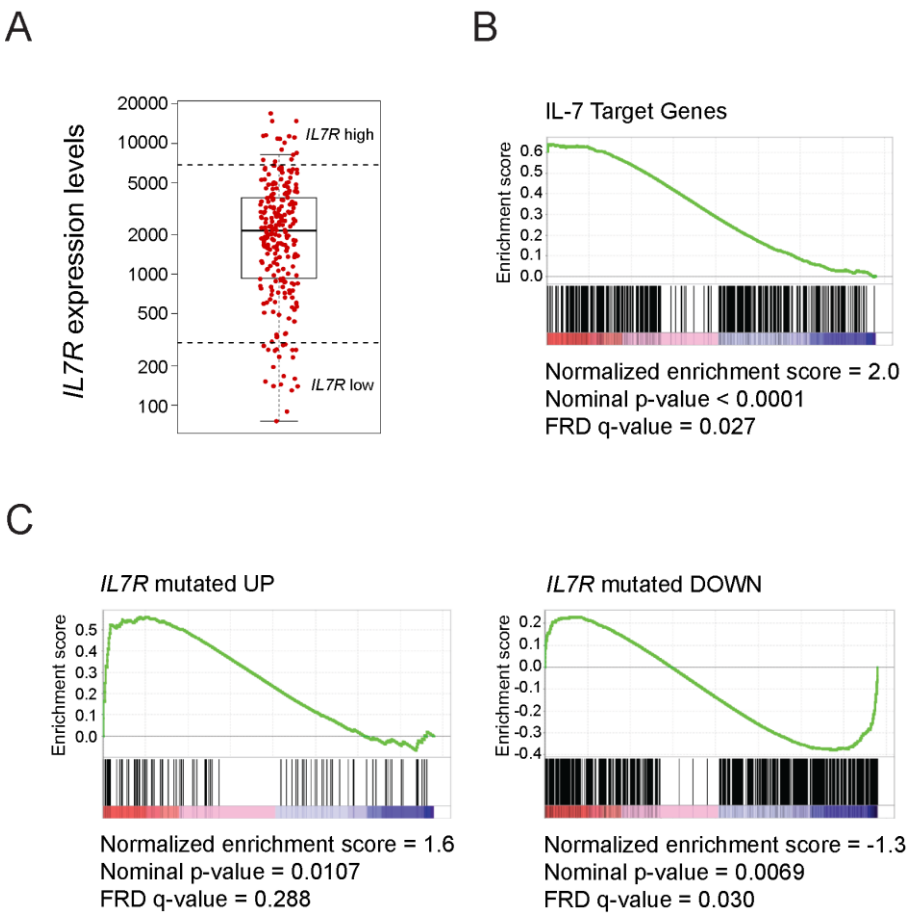
A
B
C
IL7R expression levels
20000
10000
5000
2000
1000
500
200
100
IL7R high
IL7R low
IL-7 Target Genes
Enrichment score
0.6
0.5
0.4
0.3
0.2
0.1
0.0
Normalized enrichment score = 2.0
Nominal p-value < 0.0001
FRD q-value = 0.027
IL7R mutated UP
Enrichment score
0.5
0.4
0.3
0.2
0.1
0.0
Normalized enrichment score = 1.6
Nominal p-value = 0.0107
FRD q-value = 0.288
IL7R mutated DOWN
Enrichment score
0.2
0.1
0.0
-0.1
-0.2
-0.3
-0.4
Normalized enrichment score = -1.3
Nominal p-value = 0.0069
FRD q-value = 0.030

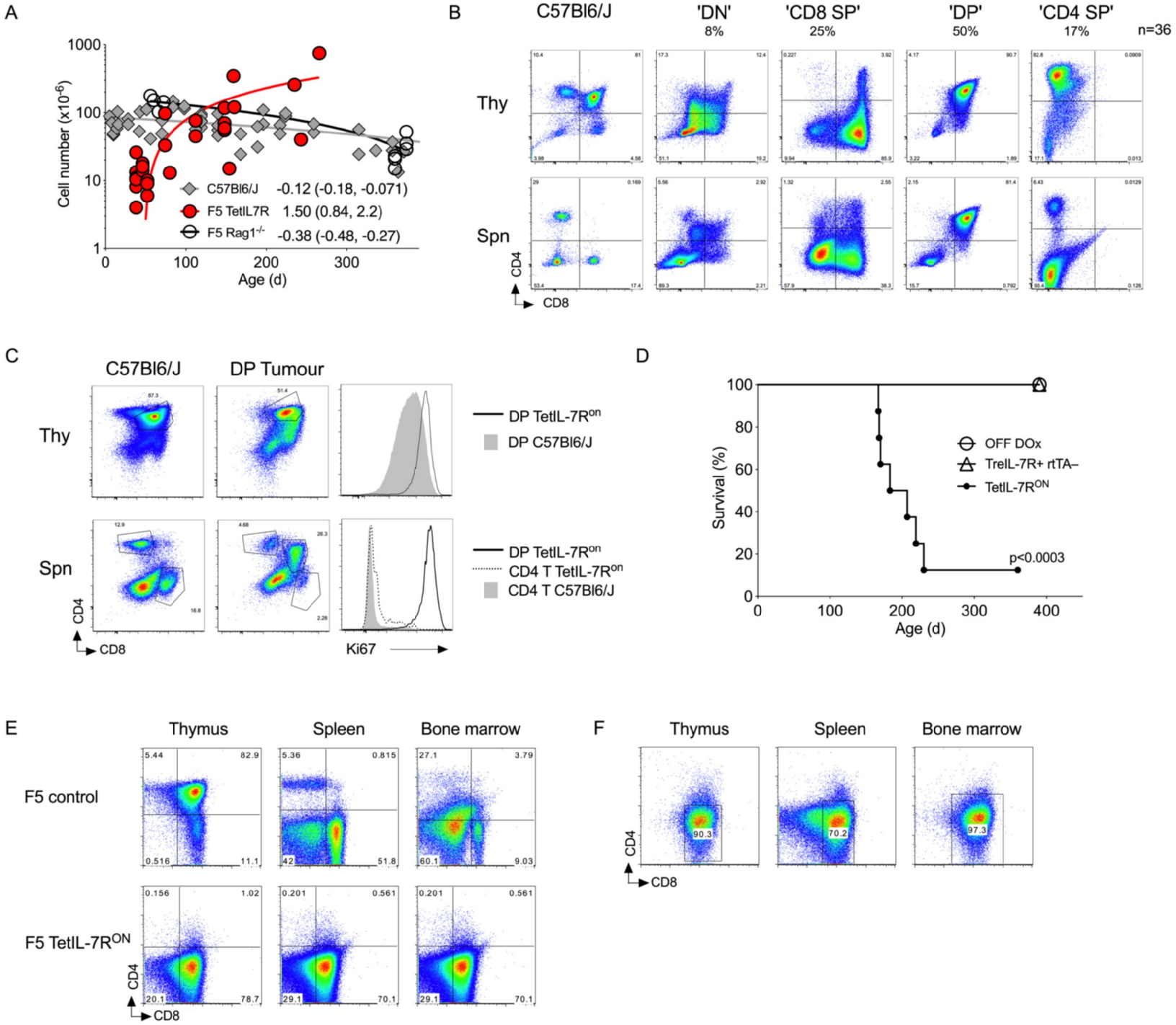
A
Cell number (x10^-6)
1000
100
10
1
0
100
200
300
Age (d)
C57Bl6/J -0.12 (-0.18, -0.071)
F5 TetIL7R 1.50 (0.84, 2.2)
F5 Rag1-/- -0.38 (-0.48, -0.27)
B
C57Bl6/J
'DN'
8%
'CD8 SP'
25%
'DP'
50%
'CD4 SP'
17%
n=36
Thy
Spn
CD4
CD8
C
C57Bl6/J
DP Tumour
Thy
Spn
CD4
CD8
Ki67
DP TetIL-7R^on
DP C57Bl6/J
DP TetIL-7R^on
CD4 T TetIL-7R^on
CD4 T C57Bl6/J
D
Survival (%)
100
80
60
40
20
0
0
100
200
300
400
Age (d)
OFF DOx
TreIL-7R+ rtTA–
TetIL-7R^ON
p<0.0003
E
Thymus
Spleen
Bone marrow
F5 control
F5 TetIL-7R^ON
CD4
CD8
F
Thymus
Spleen
Bone marrow
CD4
CD8
90.3
70.2
97.3

A

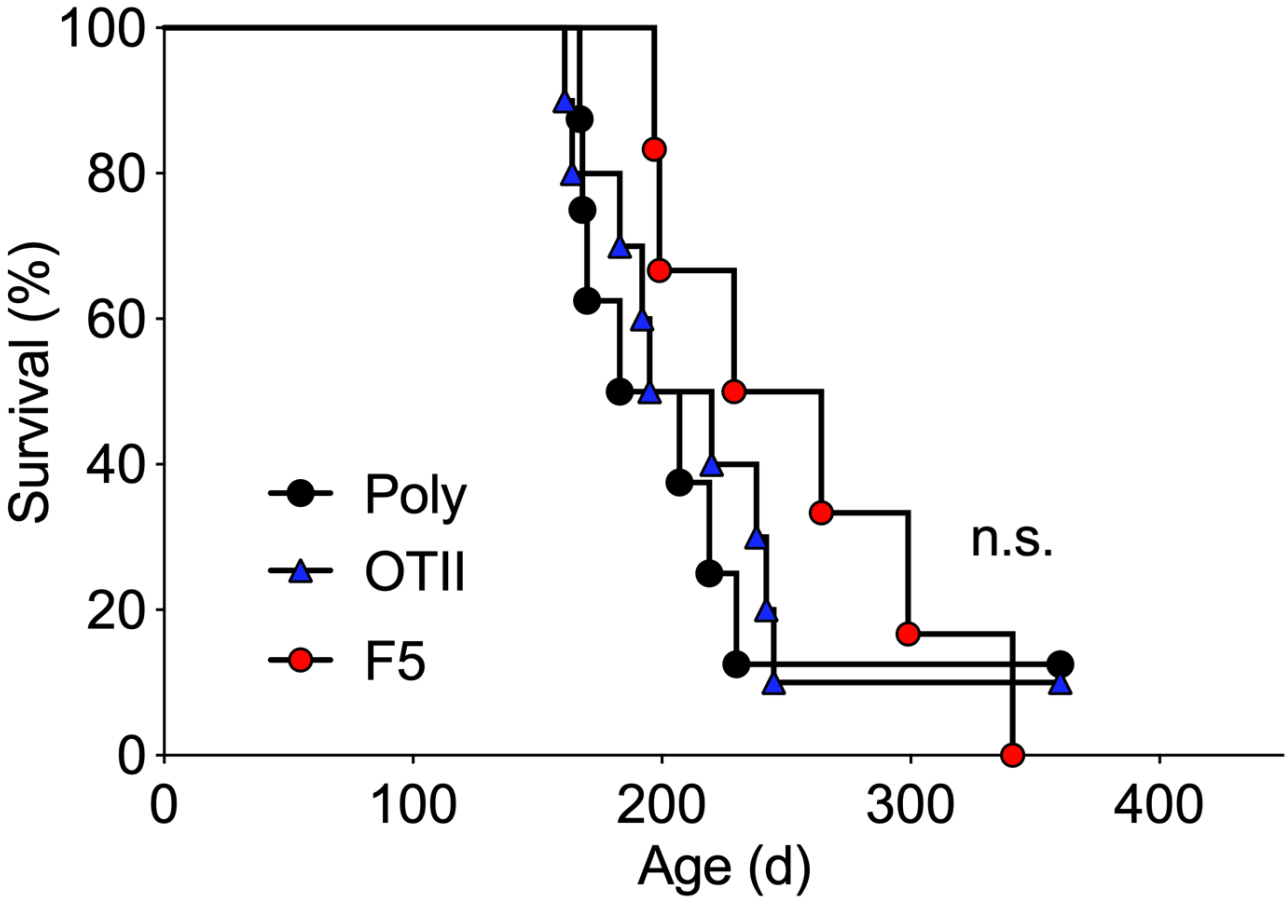
100
80
60
40
20
0
Survival (%)
Poly
OTII
F5
n.s.
0
100
200
300
400
Age (d)

B

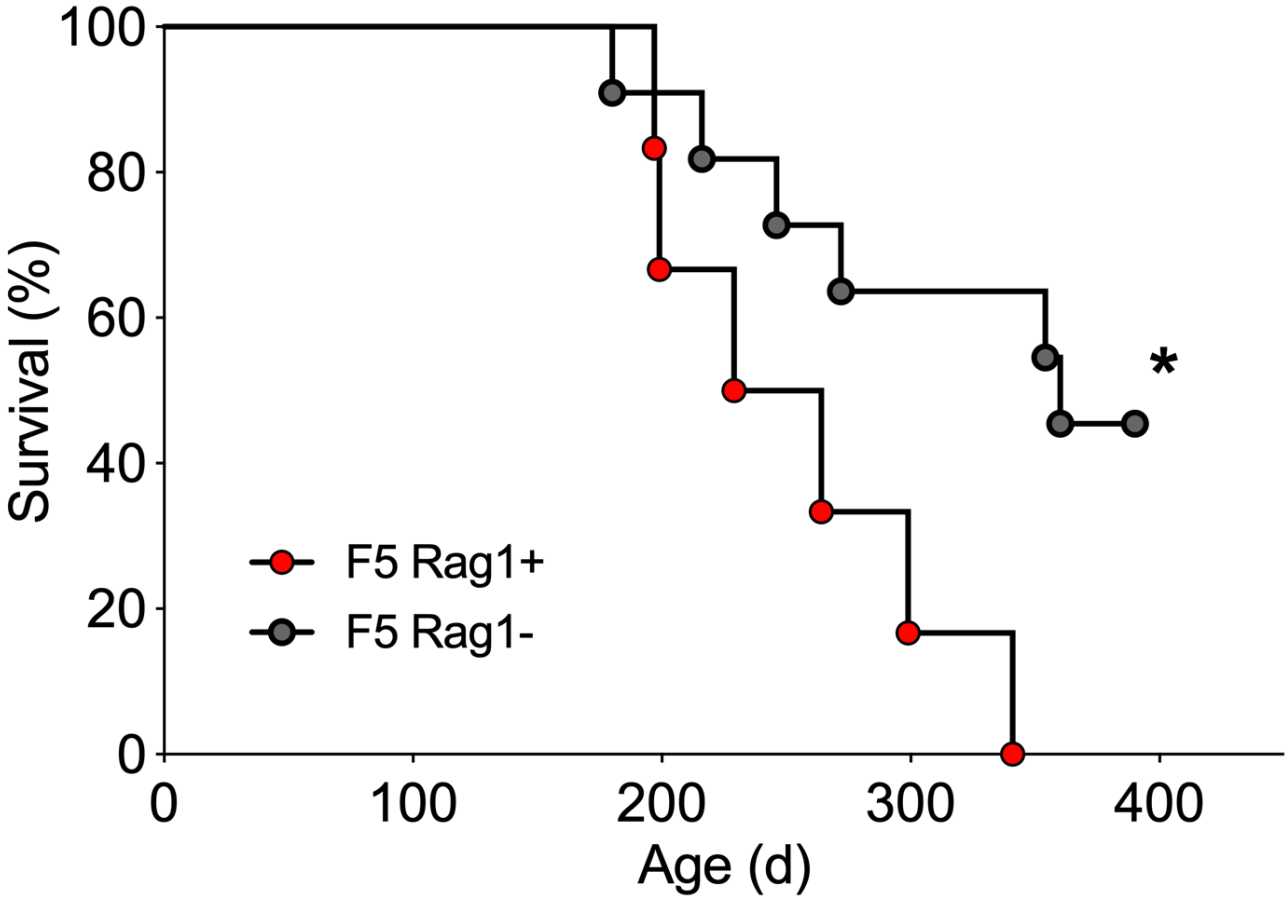
100
80
60
40
20
0
Survival (%)
F5 Rag1+
F5 Rag1-
*
0
100
200
300
400
Age (d)

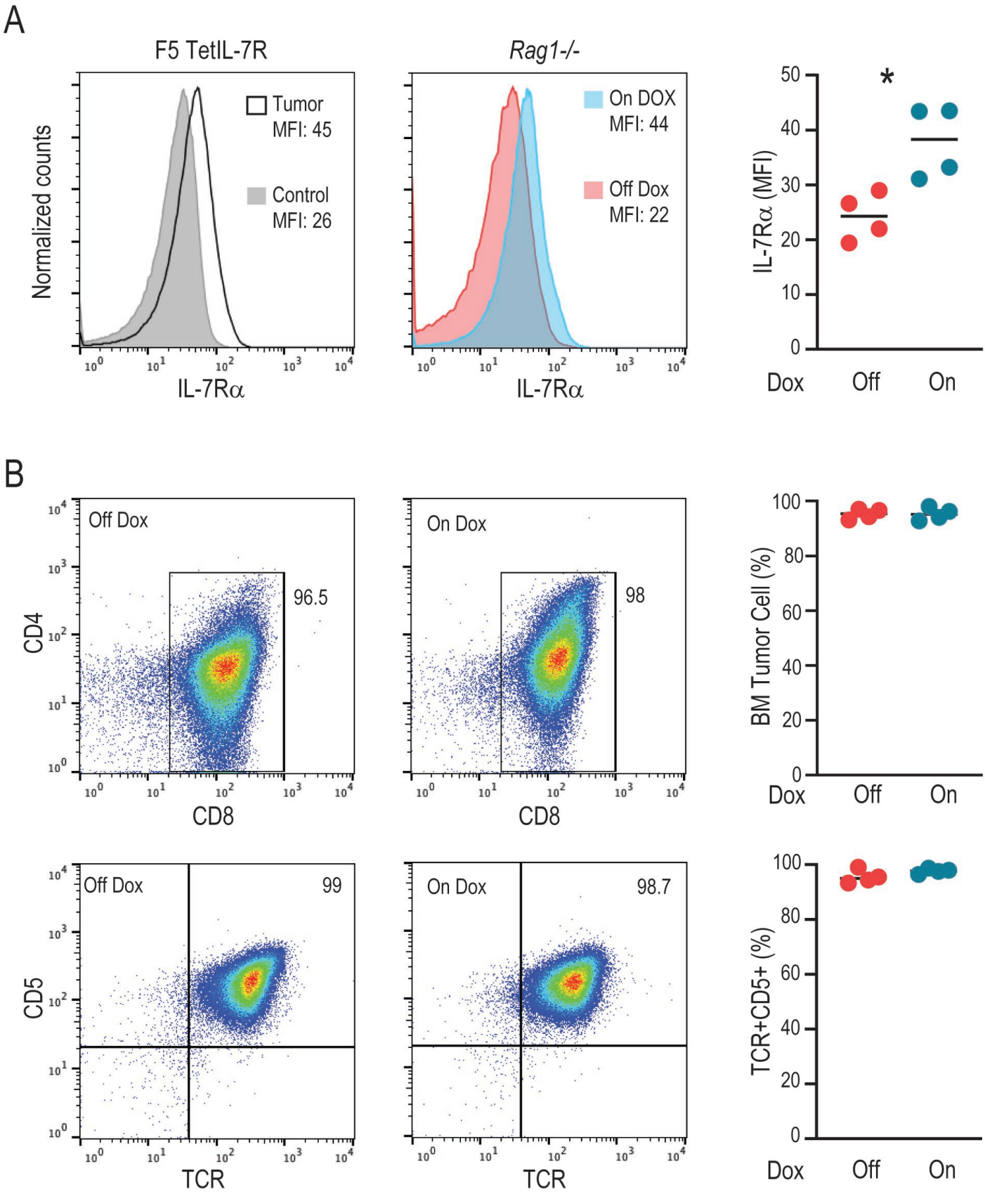
A
F5 TetIL-7R
Rag1-/-
Normalized counts
Tumor
MFI: 45
Control
MFI: 26
On DOX
MFI: 44
Off Dox
MFI: 22
IL-7Rα
IL-7Rα (MFI)
*
Dox
Off
On
B
Off Dox
On Dox
96.5
98
CD4
CD8
BM Tumor Cell (%)
99
98.7
CD5
TCR
TCR+CD5+ (%)

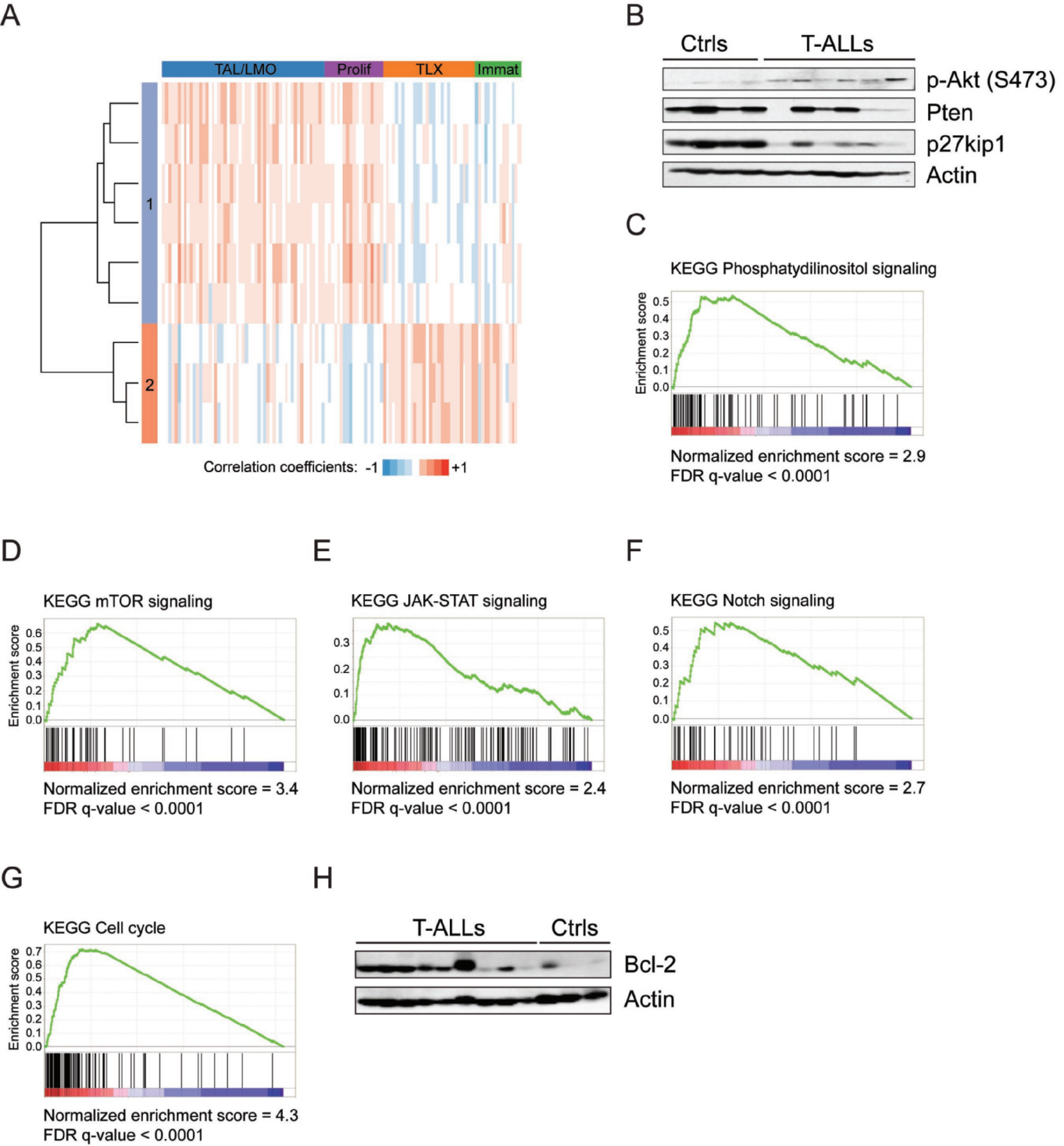
A
TAL/LMO
Prolif
TLX
Immat
1
2
Correlation coefficients: -1 +1
B
Ctrls
T-ALLs
p-Akt (S473)
Pten
p27kip1
Actin
C
KEGG Phosphatydilinositol signaling
Enrichment score
Normalized enrichment score = 2.9
FDR q-value < 0.0001
D
KEGG mTOR signaling
Enrichment score
Normalized enrichment score = 3.4
FDR q-value < 0.0001
E
KEGG JAK-STAT signaling
Normalized enrichment score = 2.4
FDR q-value < 0.0001
F
KEGG Notch signaling
Normalized enrichment score = 2.7
FDR q-value < 0.0001
G
KEGG Cell cycle
Enrichment score
Normalized enrichment score = 4.3
FDR q-value < 0.0001
H
T-ALLs
Ctrls
Bcl-2
Actin

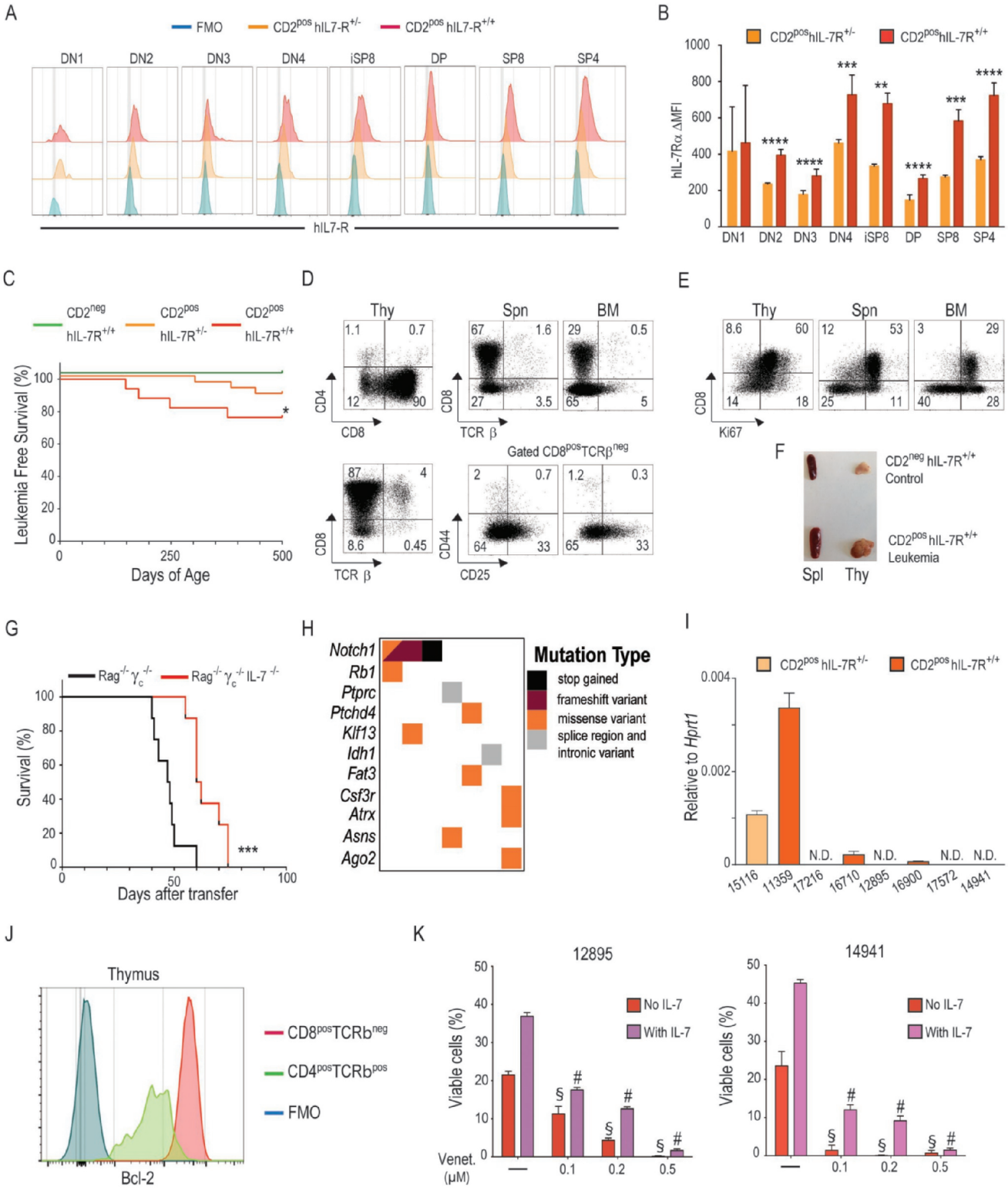
A
FMO
CD2pos hIL7-R+/-
CD2pos hIL7-R+/+
DN1
DN2
DN3
DN4
iSP8
DP
SP8
SP4
hIL7-R
B
CD2posIL-7R+/-
CD2posIL-7R+/+
hIL-7Rα ΔMFI
C
CD2neg hIL-7R+/+
CD2pos hIL-7R+/-
CD2pos hIL-7R+/+
Leukemia Free Survival (%)
Days of Age
D
Thy
Spn
BM
CD4
CD8
TCR β
Gated CD8posTCRβneg
CD44
CD25
E
Ki67
F
CD2neg hIL-7R+/+
Control
CD2pos hIL-7R+/+
Leukemia
Spl
Thy
G
Rag-/- γc-/-
Rag-/- γc-/- IL-7 -/-
Survival (%)
Days after transfer
H
Notch1
Rb1
Ptprc
Ptchd4
Klf13
Idh1
Fat3
Csf3r
Atrx
Asns
Ago2
Mutation Type
stop gained
frameshift variant
missense variant
splice region and intronic variant
I
Relative to Hprt1
N.D.
15116
11359
17216
16710
12895
16900
17572
14941
J
Thymus
CD8posTCRb neg
CD4posTCRb pos
FMO
Bcl-2
K
12895
14941
No IL-7
With IL-7
Viable cells (%)
Venet. (μM)

A

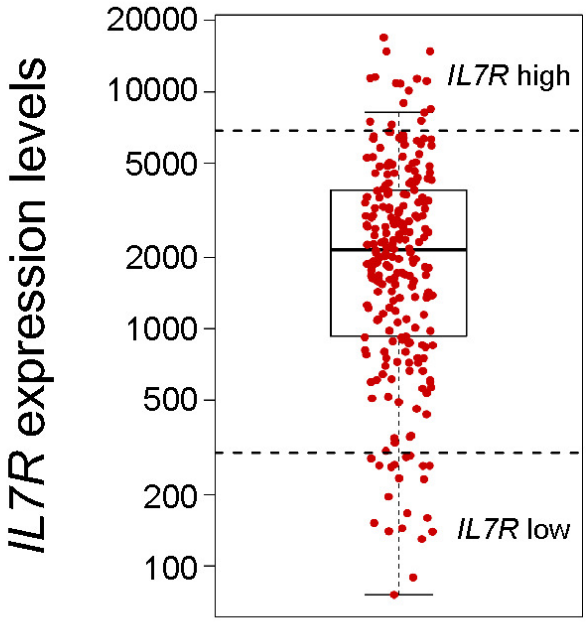

B

Normalized enrichment score = 2.0
Nominal p-value < 0.0001
FRD q-value = 0.027

C

IL7R mutated UP

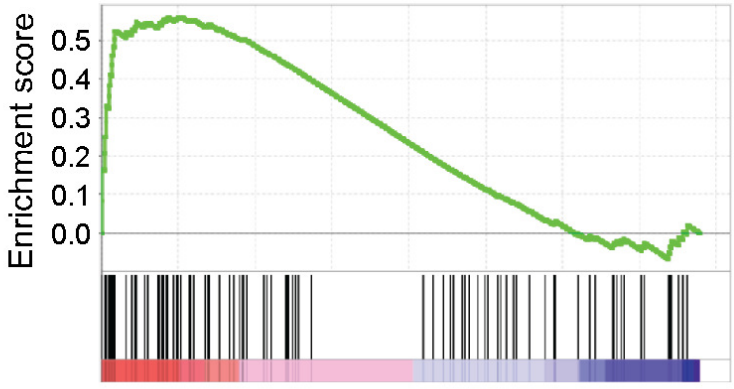

Normalized enrichment score = 1.6
Nominal p-value = 0.0107
FRD q-value = 0.288

IL7R mutated DOWN

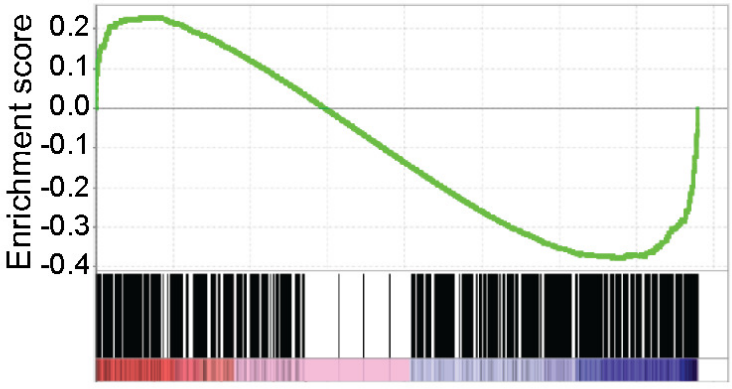

Normalized enrichment score = -1.3
Nominal p-value = 0.0069
FRD q-value = 0.030